Environmental Science
Water Research & Technology

PAPER

View Article Online
View Journal

Cite this: DOI: 10.1039/d0ew00426j

Tracking the formation of new brominated disinfection by-products during the seawater desalination process†

Leanne C. Powers, *[a] Annaleise Conway,[a] Carys L. Mitchelmore, [a] Stephen J. Fleischacker,[b] Mourad Harir,[c] Danielle C. Westerman,[d] Jean Philippe Croué,[e] Philippe Schmitt-Kopplin, [cf] Susan D. Richardson [d] and Michael Gonsior *[a]

Received 30th April 2020,
Accepted 1st June 2020

DOI: 10.1039/d0ew00426j

rsc.li/es-water

Several areas around the world rely on seawater desalination to meet drinking water needs, but a detailed analysis of dissolved organic matter (DOM) changes and disinfection by-product (DBP) formation due to chlorination during the desalination processes has yet to be evaluated. To that end, DOM composition was analyzed in samples collected from a desalination plant using bulk measurements (*e.g.* dissolved organic carbon, total dissolved nitrogen, total organic bromine), absorbance and fluorescence spectroscopy, and ultrahigh resolution mass spectrometry (HRMS). Water samples collected after chlorination (*e.g.* post pretreatment (PT), reverse osmosis (RO) reject (brine wastewater) (BW), RO permeate (ROP), and drinking water (DW)), revealed that chlorination resulted in decreases in absorbance and increases in fluorescence apparent quantum yield spectra. All parameters measured were low or below detection in ROP and in DW. However, total solid phase extractable (Bond Elut Priority PolLutant (PPL) cartridges) organic bromine concentrations increased significantly in PT and BW samples and HRMS analysis revealed 392 molecular ions containing carbon, hydrogen, oxygen, bromine (CHOBr) and 107 molecular ions containing CHOBr + sulfur (CHOSBr) in BW PPL extracts. A network analysis between supposed DBP precursors suggested that the formation of CHOBr formulas could be explained largely by electrophilic substitution reactions, but also HOBr addition reactions. The reactions of sulfur containing compounds are more complex, and CHOSBr could possibly be due to the bromination of surfactant degradation products like sulfophenyl carboxylic acids (SPC) or even hydroxylated SPCs. Despite the identification of hundreds of DBPs, BW did not show any acute or chronic toxicity to mysid shrimp. High resolution MS/MS analysis was used to propose structures for highly abundant bromine-containing molecular formulas but given the complexity of DOM and DBPs found in this study, future work analyzing desalination samples during different times of year (*e.g.* during algal blooms) and during different treatments is warranted.

Water impact

Reverse osmosis reject water collected at a desalination plant had high organic bromine concentrations and contained 519 bromine-containing disinfection by-products (DBPs) with unknown structures. Of these DBPs, we propose structures for three new brominated compounds. Despite the large number of brominated molecular formulas, reject water collected here exhibited no acute or chronic toxicity to mysid shrimp.

[a] *University of Maryland Center for Environmental Science, Chesapeake Biological Laboratory, Solomons, MD, 20688 USA. E-mail: lpowers@umces.edu, gonsior@umces.edu*
[b] *Tampa Bay Water, Clearwater, FL, 33763 USA*
[c] *Helmholtz Zentrum München, German Research Center for Environmental Health, Research Unit Analytical BioGeoChemistry, D-85764 Neuherberg, Germany*
[d] *Department of Chemistry and Biochemistry, University of South Carolina, Columbia, SC, 29208 USA*
[e] *Institut de Chimie des Milieux et des Matériaux IC2MP UMR 7285 CNRS, Université de Poitiers, 86073 Poitiers Cedex 9, France*
[f] *Technische Universität München, Chair of Analytical Food Chemistry, D-85354 Freising-Weihenstephan, Germany*

† Electronic supplementary information (ESI) available. See DOI: 10.1039/d0ew00426j

1 Introduction

While the disinfection of freshwater for drinking has been used for over one hundred years to kill waterborne pathogens, disinfection can result in the formation of disinfection by-products (DBPs).[1–3] In fact DBPs formed due to the chlorination of freshwater for drinking water have been studied for several decades.[2,3] Regulated DBPs pose known adverse health effects, such as cytotoxicity, carcinogenicity, and the disruption of the endocrine and thyroid hormone systems.[2,4–8] These DBPs are mainly halogenated organic chemicals formed by reaction of the disinfectant with natural organic matter.[2,3] However, new halogenated DBPs are found regularly with unknown toxicity to human and aquatic organisms.[9–24]

Desalination of seawater is becoming an increasingly important mechanism of meeting drinking water demands around the globe, with many desalination plants already operating in a variety of coastal locations. Continuous chlorination with chlorine concentrations <2 mg L^{-1} and contact times that range from ~15 min to a few hours or intermittent shock chlorination at higher doses are often used to disinfect incoming seawater and to control membrane fouling.[25,26] Hypochlorous acid (HOCl) is typically used in chlorination[25] but HOCl reacts rapidly with bromide (Br^-) and iodide (I^-) to form hypobromous acid (HOBr) and hypoiodous acid (HOI), respectively.[27] For example,[28]

$$HOCl + Br^- \rightarrow HOBr + Cl^- \ (k = 1.6 \text{ to } 6.8 \times 10^3\ M^{-1}\ s^{-1}) \quad (1)$$

$$HOBr \leftrightarrow OBr^- + H^+ \ (pK_a \sim 8.8 \text{ at ionic strength } 0.02 \text{ to } 0.5 \text{ and } 25\ ^\circ C) \quad (2)$$

While eqn (1) is pH and temperature dependent, given the higher pK_a of HOBr (~8.8) *versus* that for HOCl (~7.5),[28] HOBr should be a more effective disinfectant in the pH 6–8 range. HOBr reactions with organic compounds can be up to three orders of magnitude greater than those with HOCl,[28] so even in freshwaters with low bromide concentrations (*e.g.* 0.01 to 1 mg L^{-1}) HOBr may be an important reactant. Two proposed reaction pathways of HOBr with organic compounds (org-C) are electron transfer (eqn (3)) or substitution (eqn (4)).[28]

$$HOBr + Org\text{-}C \rightarrow Br^- + Org\text{-}C_{ox} \quad (3)$$

$$HOBr + Org\text{-}C \rightarrow Org\text{-}C\text{–}Br \quad (4)$$

Eqn (4) results in a brominated compound and is a Br^- sink, but eqn (3) results in an oxidized organic compound and Br^-, which allows Br^- to be available to react again with HOCl (eqn (1)). Unlike in freshwater which generally contains low μg L^{-1} concentrations of bromide and iodide, seawater bromide concentrations are ~60 mg L^{-1} at salinity 35 and iodide concentrations are ~60 μg L^{-1}.[29,30] Therefore, given the very high bromide concentrations in seawater and eqn (1)–(4), HOBr should be the active disinfectant in a desalination plant using HOCl during shock chlorination of seawater, but not during disinfection of the drinking water.

It has been shown that when HOCl is used to disinfect freshwater, mainly Cl-DBPs are formed.[14,31] However, when HOBr is used as a disinfectant (*e.g.* during shock chlorination of seawater), it is expected that numerous and new brominated DBPs are formed[32] that can be discharged to the environment. In general, brominated compounds are more toxic than chlorinated compounds and iodinated compounds are more toxic than brominated compounds,[2] but environmental toxicity has been rarely tested. Furthermore, most DBPs have not been assessed for toxicity, so this generalization is only based on a limited number of known DBPs.

Reverse osmosis (RO) is the most commonly used technology in desalination plants which results in processed drinking water but also concentrated RO brines that are often concentrated to twice the salinity of intake water when discharged back into coastal waters.[33] To date, both regulated and non-regulated DBPs have been analyzed in samples collected along a desalination treatment train.[25] For instance, DBPs regulated for drinking water (trihalomethanes, haloacetic acids, haloacetonitriles, and haloketones) were detected in desalination plants in Saudi Arabia.[32] Concentrations of each DBP were between 1 to 5 μg L^{-1} in processed drinking water,[32] which are well below US Environmental Protection Agency (EPA) guidelines for these compounds.[34] However, at a plant that used continuous chlorination of intake water with high dissolved organic carbon (DOC) levels, concentrations of these DBP compounds were quite elevated in RO brines (2 to 250 μg L^{-1}) and were relatively high (~9 to 25 μg L^{-1}) in coastal waters near the plant.[32] Because RO brines contain a mixture of chemicals, discharge could be toxic even if targeted chemicals are below threshold limits. Whole effluent toxicity testing has been used to determine the potential environmental impacts of RO brine discharge,[35] but it is still imperative to know what additional DBPs are in RO reject (brine) water (BW) when released to the environment.

As mentioned earlier there are distinct differences in the types of DBPs formed in different waters due to the presence of bromide in those containing saltwater. Furthermore, specific precursors of DBP formation in natural waters are unknown, given that dissolved organic matter (DOM) is the primary reactant and is extremely complex. Studies even demonstrated that the majority of DOM is indistinguishable across diverse environments (freshwater to marine systems) given the vast number of structural isomers for any given molecular formula.[36,37] This complexity is not surprising given that DOM in the coastal ocean may be comprised of terrestrial DOM exported from riverine systems and tidal marshes, marine DOM inputs from shelf waters, and DOM that is unique to coastal systems themselves (*e.g.* exuded from primary producers[38,39] and re-suspended from coastal sediments[40]).[41–43] DOM is also variable on spatial and

temporal scales as it is transformed and/or degraded by numerous processes including heterotrophic bacteria respiration and photochemical reactions.[44–48] To even further complicate the matter, cleaning agents like aromatic surfactants are used to control biofouling on membranes beyond using HOCl and these surfactants might be susceptible to free bromine.[49] Despite the fact that DOM character and composition will influence the nature of produced DBPs, the impact of DOM on halogenation reactions is so complex that little is known about molecular structure of the majority of newly discovered DBPs. Thus, it is likely that RO reject (brine) water (BW) contains brominated DBPs that have an unknown composition, toxicity, and reactivity.[50] Therefore, a detailed molecular characterization of DBPs formed during seawater desalination is still needed.

Non-targeted ultrahigh-resolution mass spectrometry (HRMS) and optical property analyses (absorbance and fluorescence spectroscopy) have become useful tools in evaluating complex organic mixtures such as DOM in aquatic environments. HRMS has also revealed that thousands of DBPs and organic pollutants are present in the environment.[51] Recent studies that have used HRMS to track changes in DOM during water treatment have shown that hundreds of DBPs are formed during disinfection.[14,31,52,53] Chlorine-containing DBPs had significantly more unsaturation and oxygenation than the non-chlorinated molecular formulas found before disinfection,[52] in line with expected oxidation reactions (eqn (3)) and substitution reactions on aromatic rings (eqn (4)). Similarly, while coagulation–flocculation preferentially removed reduced polyphenolic-like compounds, this treatment step did not prevent the formation of halogenated polyphenolic and aromatic acid-like DBPs upon disinfection.[14] When DOM isolates obtained from the International Humic Substances Society (IHSS) were reacted with chlorine, large decreases in UV absorbance and electron donating capacity were observed.[54] Thus, for terrestrial DOM with high aromatic content, HOCl may primarily react with phenolic and hydroquinone moieties within the DOM pool.[14,16–18] Indeed, electrophilic substitution is expected to be a dominant reaction pathway in adding halogens into DOM, especially towards compounds with high double bond equivalents[31] like structures containing aromatic rings.[54] While electrophilic substitution reactions may be less important in seawater with less terrestrial influence, over 200 Cl-DBPs were generated during the electrochlorination of algal DOM,[55] consistent with substitution or addition reactions with unsaturated fatty acids[55] and/or fatty amides.[56] Br-DBPs sampled from desalination plants in Saudi Arabia were highest at the plant with the highest intake water DOC concentration.[32] Therefore it is expected that DBPs will be highest and possibly most diverse in desalination plants that use brackish and estuarine waters with relatively high DOC concentrations, which was the case in this study.

While HRMS has been used more frequently to investigate reactions of HOCl with DOM, there have been some studies that have also focused on the reactions of HOBr with DOM. For instance, Suwannee River natural organic matter (SRNOM, IHSS) reacted far more rapidly with HOBr than with HOCl, but there was very little change in UV absorbance when reacted with HOBr.[57] The authors found that bromine was more likely to be substituted into organic structures, whereas chlorine was more likely to cleave bonds and cause larger overall changes in DOM.[57] Suwannee River fulvic acid (SRFA, IHSS) reacted with HOCl with and without bromide produced more than 450 brominated formulas that were previously unknown.[53] However, unlike the previous work with SRNOM,[57] this study suggested that ~90% of the bromine-containing formulas had chlorine-containing analogues.[53] Thus, during seawater desalination, it is still unclear what potential changes to DOM will occur and what dominant reaction pathways will occur with HOBr. During the electro-chlorination of estuarine water in ballast water treatment, >450 brominated molecular formulas were also found that had not been previously identified.[50] Brominated formulas had a similar composition to non-brominated formulas found before chlorination, suggesting that DBP precursors span a large mass range and a large range in saturation and oxygenation. However, while a similar number of Br-DBPs were found in the SRFA study by Zhang *et al.*[53] and in the ballast seawater study of Gonsior *et al.*,[50] only about half of the bromine containing formulas overlapped between studies, suggesting that the DBPs formed are highly dependent on the source of the DOM. Therefore, the purpose of this study was to evaluate the molecular composition of complex coastal DOM and its capacity to produce halogenated (possibly primarily brominated) DBPs in saline waters during desalination disinfection.

There is the potential for effluent discharged from desalination facilities to impact resident biota in the receiving water bodies. Effluent discharges may be hypersaline (up to 2-fold the receiving water salinity) and contain a complex mixture of other chemicals concentrated during the RO process from the intake waters and/or chemicals added during various processing steps in the facility *i.e.* from chlorination/dechlorination, pH adjustments, antiscaling and membrane cleaning amongst others. Therefore, each desalination plant may contain a unique effluent that contains a complex chemical richness and higher salinity effluent that may impact organisms where it is released. These concerns have been reviewed in a number of previous studies.[35,58–60]

To investigate the toxicity of desalination plant discharged effluent a number of studies have used whole effluent toxicity (WET) tests, especially short-term chronic tests that look at mortality, growth and reproductive biological endpoints in standard test species using either simulated hypersaline solutions or actual effluent discharges from desalination plants.[61,62] The determination of effluent toxicity as part of National Pollutant Discharge Elimination System (NPDES) permits usually requires these types of tests to be conducted and a number of test species may be used. These tests are

advantageous as they investigate the total toxicity of the complex mixture arising from all of chemical contaminants, not just as an additive toxicity but it also encompasses the multiple interactions in this complex mixture that may impact toxicity (*e.g.* synergism and potentiation). However, these tests are limited in their representation of the potential impacts to sensitive local species and reflect only the toxicity of the water at the time of sampling.

We conducted a preliminary study following a non-targeted approach using negative ion electrospray (ESI^-)-Fourier transform ion cyclotron resonance mass spectrometry (FT-ICR MS). Additional analyses, including water sample optical properties (absorbance and fluorescence spectra), dissolved organic carbon (DOC), total dissolved nitrogen (TDN), and total PPL extractable organic bromine (OrganoBr) were performed. Together, these techniques were used to describe in detail organic matter complexity and DBPs during the treatment train at a desalination plant located in the United States. To complement these results and especially those for BW, this water (BW) was compared against the intake/raw water (RW) using standard EPA chronic toxicity tests using the mysid shrimp. These tests determined both acute (*i.e.* mortality) and chronic (*i.e.* growth) biological endpoints and evaluate the impact of BW released back into coastal waters on resident organisms.

2 Materials and methods

2.1 Sample description and collection

Water samples were collected from a desalination plant located in the United States. This site was selected because of the potentially diverse DOM sources including two local rivers, dense coastal vegetation, and other *in situ* sources. Samples (10–20 L) were collected in duplicate at various stages during the treatment and desalination process using low density polyethylene cubitainers that had been previously cleaned with 0.1 N NaOH and rinsed several times with ultrapure MilliQ water. All containers were rinsed at least three times with sample before collection. Samples collected included intake/raw water (RW), water following pretreatment steps (PT) but before reverse osmosis (RO), RO permeate (ROP), RO reject/brine water (BW), and finished drinking water (DW) (*i.e.* ROP with additional disinfection). Pretreatment of RW entails coagulation and flocculation, sand filtration, diatomaceous earth filtration, and finally cartridge filtration (5 μm Fulflo Durabond and Honeycomb filters, Parker Hannifin Corporation).[63] After cartridge filtration, disinfection is achieved with sodium hypochlorite, and prior to RO, dechlorination is achieved with sodium bisulfite to preserve RO membranes. Post RO, both ROP and concentrated BW were collected. Finally, DW was collected post chlorination of ROP, which had a final concentration of 3.4 mg L^{-1} free chlorine. For all samples, salinity (S, unitless) was determined using a YSI Sonde according to the practical salinity scale (PSS-78).[30] Chemical and physical properties for all samples are given in Table S1.†

Samples were transported on wet ice to the Chesapeake Biological Laboratory (~48 h) and some of the RW and BW were used immediately for the toxicity tests. All other samples once received at the laboratory were filtered through 0.7 μm GF/F filters (Whatman®) that had been previously combusted for 4 h at 500 °C. Subsamples were reserved from all samples for DOC and TDN measurements, as well as for optical property analyses. To prepare and desalt the remaining samples for mass spectrometric analysis, we used a solid phase extraction (SPE) procedure. All of these procedures are described below.

2.2 DOC and TDN analyses

Filtered water samples were acidified to pH 2 using concentrated HCl (Sigma Aldrich) for DOC and TDN analysis. DOC and TDN concentrations were determined using a Shimadzu total organic carbon analyzer (TOC-V_{CPH}), and ultrapure water served as both the DOC and TDN blank. Potassium hydrogen phthalate and potassium nitrate were dissolved in ultrapure water and used as standards, respectively, between 0 and 20 mg L^{-1}.

2.3 Determination of optical properties

Samples were pipetted into a 1 cm fluorescence cuvette. Absorbance and fluorescence were simultaneously recorded at 3 nm intervals between excitation wavelengths of 230 and 550 nm using a Horiba Aqualog system. Ultrapure water served as the absorbance and fluorescence blank, and was subtracted from all scans. To generate excitation–emission matrix spectra (EEMS), a fluorescence emission spectrum was recorded at a fixed wavelength range between 230 and 597 nm (~3.3 nm intervals) for every excitation wavelength using 1–15 s integration time depending on sample absorbance. Rayleigh scattering signals were removed from all EEM spectra in Matlab® using methods described previously,[64] and any inner filter effects were corrected using the Aqualog software. EEM spectra were normalized to the water Raman scattering peak, thus all EEMS are reported in water Raman units (RU). In addition to the absorbance scans that accompany fluorescence scans, separate absorbance ($A(\lambda)$) scans were recorded for all samples between 230 and 700 nm. Raw $A(\lambda)$ spectra were corrected for any offsets by subtracting the absorbance at 700 nm from each spectrum. Corrected absorbances ($A_{corr}(\lambda)$) were converted to the Napierian absorption coefficient ($a(\lambda)$) with the following equation

$$a(\lambda) = 2.303 \times A_{corr}(\lambda)/L \quad (5)$$

where λ is the wavelength and L is the pathlength of the spectrofluorometer cuvette (*i.e.* 0.01 m).

2.4 Solid phase extraction (SPE)

DOM was isolated from samples using two in-line solid phase extraction (SPE) cartridges. Ultrapure water and aged open

ocean seawater (collected in the Sargasso Sea, May 2017) that had been reacted with chlorine for 24 h served as SPE blanks (described below). Both samples and blanks were acidified to pH 2 using concentrated ultrapure HCl (Sigma Aldrich). These samples were then drawn through clean Teflon tubing (rinsed with pH 2 ultrapure water) and connected to 1 g Bond Elut Priority PolLutant (PPL) cartridges (Agilent). PPL cartridges were activated with methanol (LC-MS Chromasolv, Sigma Aldrich) and rinsed with 0.1% formic acid water (LC-MS Chromasolv Sigma Aldrich), as described previously.[50] SPE with PPL cartridges has become a popular technique for extracting seawater DOM since PPL can retain more polar compounds than typical (*e.g.* C18, XAD) reverse phase resins.[65] However, DOC recovery is typically only 40–50% for marine DOM,[65] possibly because small organic acids and highly polar compounds are not retained using this technique. Therefore, a weak anion exchange cartridge (500 mg Oasis® WAX) was attached to each PPL cartridge to recover compounds not well retained by the PPL resin. Preliminary tests using this procedure indicated that WAX SPE is typically able to recover an additional 5% of the total DOC. WAX cartridges were activated using methanol with 2% ammonium hydroxide (Sigma Aldrich) and were rinsed with pure water. To avoid overloading the SPE cartridges with DOM, we tried to ensure no more than 10 mg carbon was placed on each PPL cartridge. Thus, depending on each sample's DOC concentration, 1 to 10 L of sample was passed through the two in-line cartridges at a rate of ~1 mL min^{-1}. Sample "breakthrough", or the water that passed through both cartridges, was collected in either clean 10 L cubitainers or in combusted 1–2 L bottles. To minimize formic acid in breakthrough samples, about ~10 mL was passed through the cartridges and discarded before collecting these samples. Breakthrough samples were analyzed for DOC, TDN, and optical properties, to determine extraction efficiencies using this SPE procedure.

After extraction, all cartridges were rinsed with at least 30 mL 0.1% formic acid water (Sigma Aldrich) and dried under the hood in a vacuum manifold. PPL cartridges were eluted with 10 mL high purity methanol and WAX cartridges were eluted with 10 mL high purity methanol with 2% ammonium hydroxide, each into individual combusted amber glass vials. Because sample pH and matrix differences in filtered water samples can impact sample optical properties, SPE-DOM samples were also prepared for analysis. To do this, 0.5 mL aliquots of the methanolic PPL and WAX extracts were dried under N_2 and re-dissolved in 5 mL ultrapure water, referred to PPL-DOM and WAX-DOM respectively. Otherwise, methanolic extracts were stored at −20 °C until mass spectrometric analysis.

2.5 Chlorination experiments

To better understand the potential for DBP formation from this diverse DOM site, we performed a chlorination experiment using RW. A 500 mg L^{-1} combusted NaCl (≥99.0%, Acros Organics) solution was chlorinated for 15 min using an electrochlorination unit (ChlorMaker saltwater chlorine generator, ControlOMatic, Inc). Free chlorine (Cl_2) concentrations were determined using HACH Method 8021 (US EPA *N*,*N*′-diethyl-*p*-phenylenediamine (DPD) method for free chlorine) with a HACH autoanalyzer and HACH free chlorine reagent for 10 mL samples. Standards were generated by diluting a 29.6 ± 0.3 mg L^{-1} low range chlorine standard solution (HACH) with ultrapure water. Free chlorine (9.7 mg L^{-1}) was added to RW samples in duplicate and reacted for 24 h. After 24 h, free chlorine concentrations were ~1.6 mg L^{-1} in reacted RW samples. While residual chlorine is typically only 0.25 to 0.5 mg L^{-1} in chlorinated seawater at desalination plants[25] instead of 1.6 mg L^{-1} measured here, we used a much higher chlorine dose (9.7 mg L^{-1}) to evaluate the maximum potential for DBP formation at this coastal site. To test for any contamination from electrochlorination solution, free chlorine (2.2 mg L^{-1}) was also added to ultrapure water as a blank, and chlorine concentrations did not change in 24 h. To dechlorinate the reacted samples, sodium thiosulfate (Sigma-Aldrich) at 2.5× the molar Cl_2 concentration was added to all samples after 24 h. Because DW had a Cl_2 concentration of 3.4 mg L^{-1} and was not dechlorinated before SPE, additional open ocean seawater and pure water samples were spiked to a final Cl_2 concentration of 3.4 mg L^{-1}. These samples were then acidified to pH 2 and underwent the same SPE procedure described above to check for any contamination from the resin. At each step in the experiment (before/after chlorination and after dechlorination) aliquots were collected for DOC and TDN measurement and for optical property analysis. After dechlorination, samples were acidified to pH 2 using concentrated HCl for solid phase extraction (described above).

2.6 Ultrahigh resolution mass spectrometry (MS) analysis

We used ultrahigh resolution mass spectrometry to characterize DOM in all samples and the possible production of DBPs formed during the desalination process. PPL extracts were diluted between 1 : 5 to 1 : 40 (depending on initial DOC concentrations) with ultrapure methanol and WAX extracts were diluted 1 : 2 with ultrapure methanol prior to analysis with a Bruker Solarix 12 Tesla Fourier transform (FT) ion cyclotron resonance (ICR) mass spectrometer. Ionization was achieved using negative ion mode electrospray ionization (ESI) with spray voltage set to −3.6 kV. The flow rate was held constant at 2 μL min^{-1} and 1000 scans were averaged. The autosampler was programmed to wash with 600 μL of 80 : 20 MeOH : water to prevent carryover, and blank methanol samples were injected approximately every 10 samples. The FT-ICR mass spectrometer was pre-calibrated using known arginine clusters and post-calibrated using known DOM *m*/*z* ions.[66] Exact molecular formulas (mass error <0.5 ppm) were assigned using proprietary software, which is based on the combinations of the elements $^{12}C_{1-\infty}$, $^{1}H_{1-\infty}$, $^{16}O_{1-\infty}$, $^{14}N_{0-10}$,

$^{32}S_{0-2}$, $^{35}Cl_{0-5}$, $^{79}Br_{0-5}$, $^{127}I_{0-5}$, as well as the ^{13}C, ^{34}S, ^{37}Cl and ^{81}Br isotopologues.[67,68] Additional parameters, like oxygen to carbon (O/C) ratio, hydrogen to carbon (H/C) ratio, double bond equivalent (DBE), and average carbon oxidation state (Cos), were calculated as described previously[69–71] and compared between samples using intensity weighted averages. Formula assignments with double bond equivalents (DBE) < 0, non-integer DBE values, O/C > 1 and H/C < 0.3 were excluded from the dataset. For masses with multiple assigned molecular formulas, DBE minus oxygen (DBE-O) values and expected isotopologues were used to validate one formula assignment as described previously.[67,68] Thus, validated molecular formulas only contained elemental combinations of C_{2-38}, H_{2-58}, O_{1-20}, N_{0-3}, S_{0-2}, Cl_{0-3}, Br_{0-3}, and I_{0-1}.

Molecular formula assignments with Cl and Br were confirmed manually using isotope simulation in the Bruker data analysis software as previously described in Gonsior *et al.*[50] Isotope simulation allows for confirmation of the ^{37}Cl isotopologue at 24.22% natural abundance and the ^{81}Br isotopologue at 49.31% natural abundance. Molecular formulas containing iodine cannot be confirmed using isotope simulation because ^{127}I has only one stable isotope. Assigned molecular formulas were considered valid if isotopic *m*/*z* ions were within 10% of the expected intensity based on ^{37}Cl isotopic abundance and ^{81}Br isotopic abundance. In complex organic mixtures (*i.e.* DOM), it is difficult to predict exact structures for compounds due to the large numbers of possible isomers for any given molecular formula. This structural complexity even may prevent production of useful information from fragmentation experiments (MS/MS).[36,37] However, high intensity low *m*/*z* brominated compounds were selected for fragmentation experiments to potentially elucidate structures of these unknown DBPs.

MS/MS was conducted using direct infusion of samples into a LTQ Orbitrap XL mass spectrometer (Thermo) in negative ion mode ESI, with high purity helium as the collision gas. High intensity ions from FT-ICR MS experiments with brominated formula assignments were fragmented within a 1.0 *m*/*z* window at 60 000 resolution and a maximum injection time of 150 ms. Collision energy was varied between 10 and 40 eV. BW PPL extracts were diluted 1 : 40, and BW WAX extracts were diluted 1 : 3 with pure methanol prior to analysis. MS/MS spectra were further analyzed using SIRIUS 4 software[72] to predict potential structures of DBP precursor ions and their fragments.

Throughout this study, molecular ion relative abundances and intensity-weighted average (wt) characteristics were used to compare formula assignments between samples. Van Krevelen or elemental diagrams[73] and modified Kendrick plots[55,74] were used to visualize FT-ICR MS data. Van Krevelen diagrams are plots of H/C ratios *versus* O/C ratios for all assigned molecular formulas, revealing bulk properties like the degree of saturation and oxygenation.[73] Modified Kendrick diagrams are plots of the Kendrick mass defect (KMD)[75] normalized to the *z*-score (*z**) *versus* exact mass (*m*/*z*).[74,76] KMD/*z** *versus* *m*/*z* can be used visualize homologous series of formulas based on CH_2 spacing in the horizontal direction, $-CH_4/+O$ spacing in the vertical direction, and H_2 spacing in the diagonal direction.[55,74,76] To explore possible bromination reactions, mass difference networks were created following methods described previously.[55,77] Briefly, validated assigned molecular formulas were used to construct a mass difference network where precisely measured ion masses with assigned molecular formulas (nodes) were connected by mass differences (edges). The mass differences tested were Br substitution reactions ($-H/+Br$ = 77.91051 amu) and HOBr addition reactions (95.92108 amu) and visualized using the open-source Gephi software (version 0.9.2).

2.7 Total PPL extractable organic bromine (OrganoBr) analysis

OrganoBr was determined for SPE-DOM samples using a triple quadrupole-inductively coupled plasma-mass spectrometer (ICP-MS/MS, Agilent 8900 ICP-QQQ) in no reaction gas mode. Prior to analysis, PPL extracts were diluted 10 000 times with pure water containing 0.5% ammonium hydroxide. Br was determined using *m*/*z* 79 and an integration time of 0.5 ms, 1 point per peak, 3 replicates, and 50 sweeps per replicate. The ICP mass spectrometer was tuned daily using a multi-element tuning solution containing Li, Co, Y, Tl, and Ce (Agilent), diluted to 1 μg L^{-1} with pure water. Pure ^{59}Co was used as an internal standard in all samples, blanks, and standards, which were diluted to a final concentration of 0.5 μg L^{-1}. Br standard curves were prepared in ultrapure water up to 15 μg L^{-1} added Br using 5-bromo-3-iodobenzoic acid (Sigma-Aldrich). A 1 μg L^{-1} Br solution made from NaBr (≥99.0%, Sigma) was also analyzed to assess the accuracy of bromide determinations and was within 3% (n = 3) of expected concentrations. The detection limit, defined as 3 times the standard deviation of the blank (n = 10) was 0.03 μg L^{-1} for Br. Because we did not remove inorganic Br from filtered samples, we did not determine extraction efficiency for OrangoBr.

2.8 Chronic toxicity tests

Americamysis bahia (mysid shrimp) 7 day-static renewal chronic tests were performed under the EPA whole effluent toxicity (WET) test guidelines for method 1007.0: mysid, *Mysidopsis bahia*, survival, growth, and fecundity test. Chronic toxicity was assessed using the raw water (RW) and reject (brine) water (BW).[78] *A. bahia* were shipped from Aquatic Biosystems (Fort Collins, CO) overnight the day before initiation at approximately 6–7 days old and were slowly acclimated to laboratory conditions (*i.e.* temperature and to a lesser extent salinity as they were pre-acclimated to similar salinity conditions by the supplier). Mysids were fed live brine shrimp (*Artemia* spp.) twice daily at approximately 75 *Artemia*/mysid/feeding. For both tests, artificial seawater

(ASW at S = 22.5; prepared with deionized (DI) water and Crystal Sea Marine Mix salts) aged a minimum of 24 h was used as the dilution water and negative control. Exposures were carried out in 250 mL glass jars that were conditioned with ASW before use and contained 150 mL per vessel of exposure water. Positive controls consisted of various concentrations of potassium chloride (KCl) from 0.3 to 0.7 g L^{-1} which is in the toxicity range that has been reported in previous studies.[79–82] Exposures were carried out at 26 ± 1 °C using a 16 hour light : 8 hour dark lighting regime.

For the exposures, the water being tested (RW or BW) was diluted with the dilution water (*i.e.* ASW as described above) to prepare 5 concentrations of the initial water (*i.e.* 100, 50, 25, 12.5 and 6.25%) plus a dilution water control with 8 replicates per test concentration. Tests were run at a salinity of 22.5 to match the intake RW at the time of sampling so that salinity alone was not a driver of toxicity. Our approach was similar to those conducted by Bodensteiner *et al.*[61] who also adjusted the salinity of the brine effluent from 47 to 30. BW to start was at a salinity of 60 and so was first brought down to a salinity of approximately 22.5 using DI water before exposure dilutions were prepared as described above (*i.e.* diluted 1.15 L BW to 3.15 L using DI water; effectively starting the WET test at a 36.5% dilution). Solutions were remade and renewed every 48 h. To initiate the exposure, *A. bahia* were selected indiscriminately and put into each vessel until each vessel totaled 5 mysids. During the test, visual observations were made daily noting any dead or visibly lethargic individuals, as well as confirming vessel counts. Water quality measurements (*i.e.* temperature, dissolved oxygen, pH, salinity, conductivity) were also performed daily on at least 2 replicates of the previous day/aged waters before renewal, which were rotated throughout the exposure, as well as on all new exposure solutions prepared. Any extreme deviations in water quality discussed above were addressed immediately. At the termination of the tests (day 7) all organisms in a vessel were immobilized in DI water, counted and visualized through a dissecting microscope to assess sex and to look for the presence of eggs in the females. Very few gravid females were present and so as the test did not meet the control criteria for the presence of eggs, this endpoint was not used. After microscopic analysis, all mysids present in a vessel were then placed in a foil tray and dried at 60 °C for 24 hours in a drying oven and dry weights were recorded. Statistically significant endpoints for growth and survival were determined using the EPA WET Analysis Spreadsheet (v1.6.1). Endpoints include, LC50s (effluent concentration that results in mortality to 50% of test organisms), IC25s (effluent concentration which causes a 25% reduction in growth of test organisms) and NOECs (the no observed effect level; the effluent concentration that is not statistically significantly different from the control). All tests met the minimum test acceptability criteria (*i.e.* control survival was >80% and average control dry weight of at least 0.20 mg per mysid) and water quality parameters were within those stated in the EPA guidelines for this test (see Tables S4 and S5† for details).

3 Results and discussion

3.1 Bulk properties of water samples

Filtered water sample characteristics are given in Table S1.† RW and PT had a salinity of 22.5, whereas the salinity of BW was almost three times higher at 60. It should be noted that the final effluent was not sampled, so the salinity of discharge is much lower than the BW sample. The salinity of 22.5 in RW indicates a substantial contribution of freshwater and renders this intake water more brackish than coastal waters used for desalination in more arid regions such as Saudi-Arabia or Australia. Pretreatment caused a slight reduction in DOC concentration from 4.3 mg L^{-1} in RW to 3.9 mg L^{-1} in PT, but TDN concentrations were not significantly different (Table S1†). Electrochlorination of RW resulted in little reduction in DOC concentration, but TDN values were below detection. As expected, BW had the highest DOC and TDN concentrations of 10 mg L^{-1} and 0.68 mg L^{-1}, respectively, and DOC and TDN concentrations were below detection in ROP and DW.

Optical properties revealed significant changes in all samples. Pretreatment and electrochlorination resulted in a reduction in absorption and fluorescence spectra and changes to spectral shape (Fig. 1 and Table S1†). For instance, absorbance in the visible was removed or greatly diminished in the PT and RW + Cl_2 samples when compared to RW, with higher absorbance losses at higher (*e.g.* visible) wavelengths. These changes corresponded to increases in absorption spectral slopes of 0.019 nm^{-1} in RW, 0.024 nm^{-1} in PT, and 0.029 nm^{-1} in RW + Cl_2, which were determined between 300 and 500 nm ($S_{300–500}$). Similar to DOC concentrations, BW had the highest absorption spectrum but its $S_{300–500}$ value was the same as PT (Fig. 1). Specific UV absorbance (SUVA) was also highest in RW (2.8 L mg^{-1} m^{-1}) and decreased to 1.9 L mg^{-1} m^{-1} in PT and BW. The similarities between $S_{300–500}$ and SUVA between PT and BW suggests that they have a similar composition despite much higher DOC concentrations and absorption spectra in BW. On the other hand, absorbance values were very low in both ROP and DW, but DW had a peak in its spectrum similar to that of nitrate.[83] Nitrate concentrations were not measured but TDN levels were below detection, so this absorbance peak is probably not due to nitrate. Because absorbance was low in the UV and below detection at wavelengths >400 nm in ROP and DW, the origin of this potential absorbing chromophore was not further investigated (Fig. S1†) and $S_{300–500}$ and SUVA values were not determined.

EEM spectra also showed differences among samples. The RW EEM spectrum is typical of other estuarine environments,[84] exhibiting relatively high fluorescence with excitation in the UV-visible and emission in the visible light spectrum (Fig. 1). Fluorescence loss from RW was much larger in RW + Cl_2 than in PT (Fig. 1), but loss was not uniform across emission wavelengths (Fig. S2†). Greatest fluorescence loss (~45–50%) in PT occurred between excitation wavelengths 260 nm to 340 nm and emission

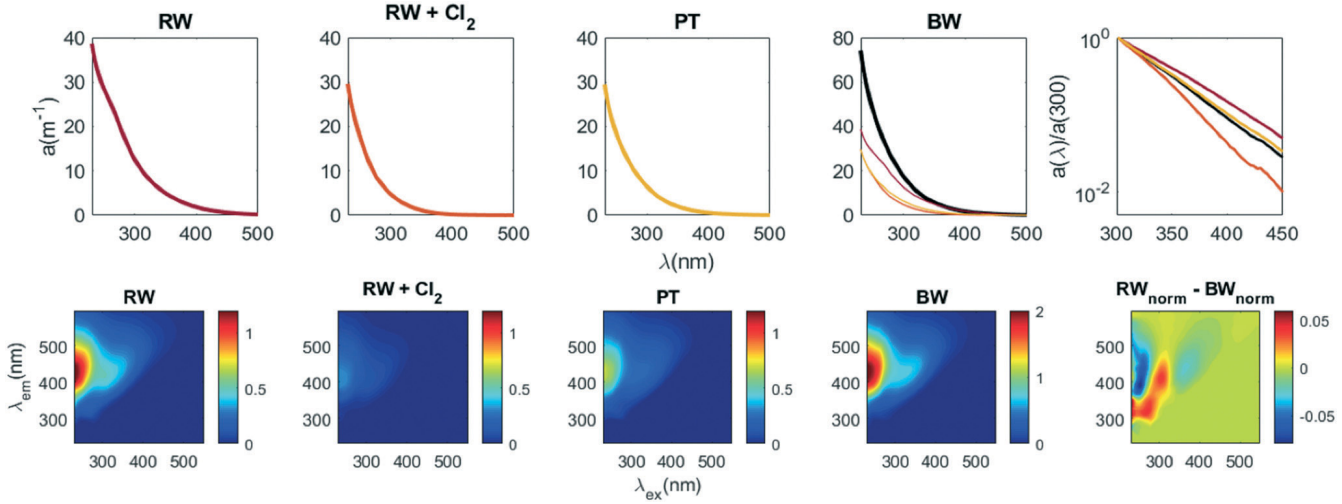

Fig. 1 Absorption spectra (a (m^{-1})) (top) and excitation–emission matrix spectra (EEMS) (water Raman units, RU) (bottom) for raw water (RW), chlorinated RW (RW + Cl_2), post pretreatment water (PT), and reject (brine) water (BW). RW (maroon line), RW + Cl_2 (orange line) and PT (yellow line) a (m^{-1}) spectra are shown with the BW spectrum (black line). The last top panel shows all a (m^{-1}) normalized to 300 nm and plotted on a log scale to highlight spectral slopes; same colors apply. The last bottom panel is a difference EEM spectrum between RW and BW (normalized to their maximum fluorescence) to highlight differences in spectral shape between RW and BW.

wavelengths 320 and 420 nm (Fig. S2†). To visualize the difference between RW and BW EEM spectra, EEM spectra for RW and BW were normalized to their maximum fluorescence intensity and subtracted (Fig. 1), revealing a similar pattern as the difference between RW and PT. Thus, like absorbance spectra, BW had the highest fluorescence but a similar shape to PT. The similarities in optical properties between BW and PT are supported by their similar fluorescence apparent quantum yield (AQY) spectra (Fig. S2†). Above ~300 nm, BW and PT have higher fluorescence AQY values than RW, with the greatest differences between 350 and 450 nm (Fig. S2†). This result suggests that absorbance between 350 and 450 nm is more greatly decreased in PT/BW samples than fluorescence over the same wavelength range. Otherwise, fluorescence in the visible light spectrum was entirely removed in ROP and DW samples (Fig. S1†), and only a very low UV fluorescence was detected, which was expected from RO treatment.

Absorption spectral slopes have been inversely correlated to average DOM molecular weight[85] and SUVA values have been correlated to DOM aromatic content.[86] Thus, the increases in spectral slope and decreases in SUVA observed between RW and PT/BW may correspond to decreases in DOM molecular weight and aromaticity. While the sources and chemical properties of high absorbance values in the visible and fluorescence spectra with large Stoke's shifts (*i.e.* humic-like fluorescence) within the ocean are still debated, in estuarine waters these features are typically correlated with terrestrial inputs.[87] These unusual properties have been proposed to arise from charge-transfer interactions between electron-rich donors (*e.g.* aromatic hydroxyl and methoxy groups) and electron-deficient acceptors (*e.g.* carbonyl groups), formed through partial oxidation of lignin, tannins, and other polyphenols.[88–90] Whether HOBr leads to oxidation or electrophilic substitution may depend on hydroxyl group position and pH, but electrophilic aromatic substitution accounted for ~20% of the bromine incorporation in SRNOM.[91] It is possible that halogenated phenolic compounds have lower electron donating capacity than non-halogenated phenolic compounds, which may partly explain the changes in optical properties between RW and PT/BW. However, oxidation reactions and/or polymerization reactions of unstable quinones have also lead to increases in absorbance spectra.[91] Therefore, it is unclear from fluorescence and absorbance spectra alone what are the major pathways of HOBr reactions with DOM in this study.

3.2 SPE-DOM properties and chemodiversity analyzed by ultrahigh resolution mass spectrometry

DOC extraction efficiencies for RW, PT, and BW samples ranged from 40 to 60% (Table S1†), which is typical for aquatic DOM.[65] Although extraction efficiencies are low for DOC, it has been noted that those for optical properties are higher for reverse phase sorbents so that PPL SPE is especially good at recovering long wavelength absorbance and humic-like fluorescence.[92] Absorption spectra for SPE-DOM samples (PPL + WAX extracts) almost quantitatively match those for original water samples for RW and PT at wavelengths >300 nm, but absorbance values of SPE-DOM for BW were significantly lower than those for original water samples across all wavelengths <400 nm (Fig. S1†). In these samples, WAX SPE recovered UV absorbance (<320 nm) that was not retained by PPL (Fig. S1†). WAX SPE blanks (extracted Milli-Q water) and ROP and DW WAX-SPE samples did not exhibit any observable absorbance. Likewise, EEM spectra of PPL SPE-DOM samples have similar shapes to whole water samples (Fig. S1 *versus* S3†), but WAX SPE-DOM

(Fig. S4†) exhibits "humic-like" fluorescence with excitation <400 nm and emission between 300 and 500 nm, indicating that some fluorescent DOM is missed by using PPL SPE alone.

With the exception of ROP and DW samples, the molecular composition of PPL SPE-DOM was diverse across all samples (Table S2 and Fig. S3†), with a high abundance of molecular formulas containing only carbon, hydrogen, and oxygen (CHO, n = 1160 to 1908), those containing CHO + nitrogen (CHNO, n = 723 to 1429), and those containing CHO + sulfur (CHOS, n = 328 to 462). CHO formula assignments for RW, PT, and BW PPL samples occupy a large area within van Krevelen space (Fig. S3†) and had a similar center of mass (~463 Da), O/C_{wt} of 0.49 to 0.55, H/C_{wt} of 1.13 to 1.17, and DBE_{wt} of ~10 (Table S2†). Intensity-weighted average carbon oxidation state (Cos_{wt}) was <0 for these samples, indicating many reduced formulas, but covered a large range of oxidation states (*e.g.* RW $Cos_{wt} = -0.18 \pm 0.34$). The relative abundance of m/z ions were also compared between RW and BW samples and plotted as either relatively increasing in BW or relatively decreasing in RW (Fig. 2). CHO formulas that relatively increased in BW were highly oxygenated (O/C ~0.7) and saturated (H/C ~1.3) with relatively low DBE values (Fig. 2A). There were many long homologous series in KMD/z* plots, suggesting that many of these signatures are highly related (Fig. 2A). CHO formulas that decreased in RW relative to BW spanned a large range, but also formed long homologous series in KMD/z* plots. These assignments had either low O/C ratios (~0.3) and high H/C ratios (~1.3) or high O/C ratios (~0.6) and low H/C ratios (~0.8). It is not surprising that this second pool of formulas decreased, since polyphenolic compounds are generally unsaturated and oxygenated[93] and electrophilic aromatic substitution is a suspected mechanism for the incorporation of bromine into DOM.[57,91]

FT-ICR MS also revealed that PT and BW PPL-SPE samples had 384 and 392 formula assignments containing CHO + bromine (CHOBr), respectively (Fig. S3 and Table S2†). These formula assignments were confirmed using isotope simulation (Fig. S6 to S10†). CHOBr in BW had an O/C_{wt} of 0.53 and a H/C_{wt} ratio of 1.12 (Table S2† and Fig. 2B), which is also consistent with the pool of CHO formulas that decreased in RW. While ESI is not uniform and not all compounds are ionized by negative-mode ESI, only 4 CHOBr molecular ions were found in RW PPL-SPE samples. These results suggests that a large number of brominated DBPs were formed during the desalination process due to the almost instantaneous conversion of HOCl to HOBr in the presence of bromide. OrganoBr concentrations in PT and BW PPL extracts were also very high relative to RW PPL extracts (Table S1†). PT SPE-DOM had an OrganoBr concentration of 330 μg L^{-1} and BW SPE-DOM had an OrganoBr concentration of 570 μg L^{-1} (Table S1†). The rapid conversion of HOCl to HOBr and subsequent reaction with DOM in RW was also observed during the laboratory-based addition of electrochlorinated water to RW, which increased the OrganoBr concentrations in RW by over a factor of 10 from 25 μg L^{-1} to 310 μg L^{-1} (Table S1†).

While there were larger differences in CHNO assignments between RW and BW (Fig. S5 and Table S2†), CHNO formulas generally followed the same trend as CHO formulas, where formulas with higher O/C ratios and higher H/C ratios relatively increased in BW and formulas over a wide range relatively decreased in RW (Fig. 2C). However, very few CHNOBr formulas were found in BW PPL extracts (Fig. 2D). A previous study found >200 chlorine-containing CHNO (CHNOCl) formulas produced from the chlorination of algal DOM.[55] The production of CHNOBr from chlorination of algal DOM in the presence of bromide has yet to be tested, but it is possible that CHNOBr formulas could become more prevalent in reject water during algal bloom events. The largest differences between RW and BW were observed in the CHOS pool, where only 4% of assignments were unique to RW but 32% of assignments were unique to BW (Fig. S5 and Table S2†), suggesting a source during water treatment. Additionally, 112 CHOSBr formulas were found in the PT (107 formulas) and the BW (108 formulas) PPL extracts (Table S2† and Fig. 2F). This CHOSBr pool was generally less oxygenated (O/C_{wt} ~0.4) and more saturated (H/C_{wt} ~1.23) than the CHOBr pool (Table S2†). DBE values of CHOS formulas that increased in BW and decreased in RW (Fig. 2E) did not follow a clear pattern like CHO formulas (Fig. 2A). However, CHOSBr pool fell in a narrow range of O/C *versus* DBE values and all CHOSBr formulas had DBE-O values between −1 to 3. These results are consistent with the bromination of CHOS formulas that relatively decreased the most in RW, which had DBE-O values from 2 to 4 (Fig. 2E). Furthermore, a large proportion of CHOS formulas were unique to PT/BW compared to RW, as mentioned above (Fig. S5 and Table S2†). The CHOS formulas that increased in BW had relatively high O/C values centered from 0.4 to 0.8 and high H/C ratios from 1 to 1.6 (Fig. 2E).

To further explore the possible reaction mechanisms between HOBr and DOM in RW, theoretical mass difference networks were created tracking both substitution reactions (–H/+Br) and addition reactions (+HOBr) between both CHO and CHOS formulas (Fig. 3 and S12,† respectively). For CHO formulas, both substitution reactions and addition reactions can explain the formation of all brominated compounds in BW (Fig. 3, $C_{18}HO$ formulas highlighted as an example). However, these reactions can only partly explain the formation of CHOSBr compounds (Fig. S12†). Bromine incorporation into the aromatic rings of commercial surfactants like linear alkylbenzene sulfonates (LAS) has been demonstrated,[49] as well as the hydroxylation of the aromatic ring during reactions of HOCl/HOBr.[49] To explore this possibility in our dataset, hydroxylation and Br substitution (–2H/+Br/+OH and –H/+Br) were tested for suspected surfactant molecular ions using the mass difference network analysis. This approach revealed that a portion of the CHOSBr pool may be formed from bromine substitution on the aromatic rings of suspected sulfophenyl

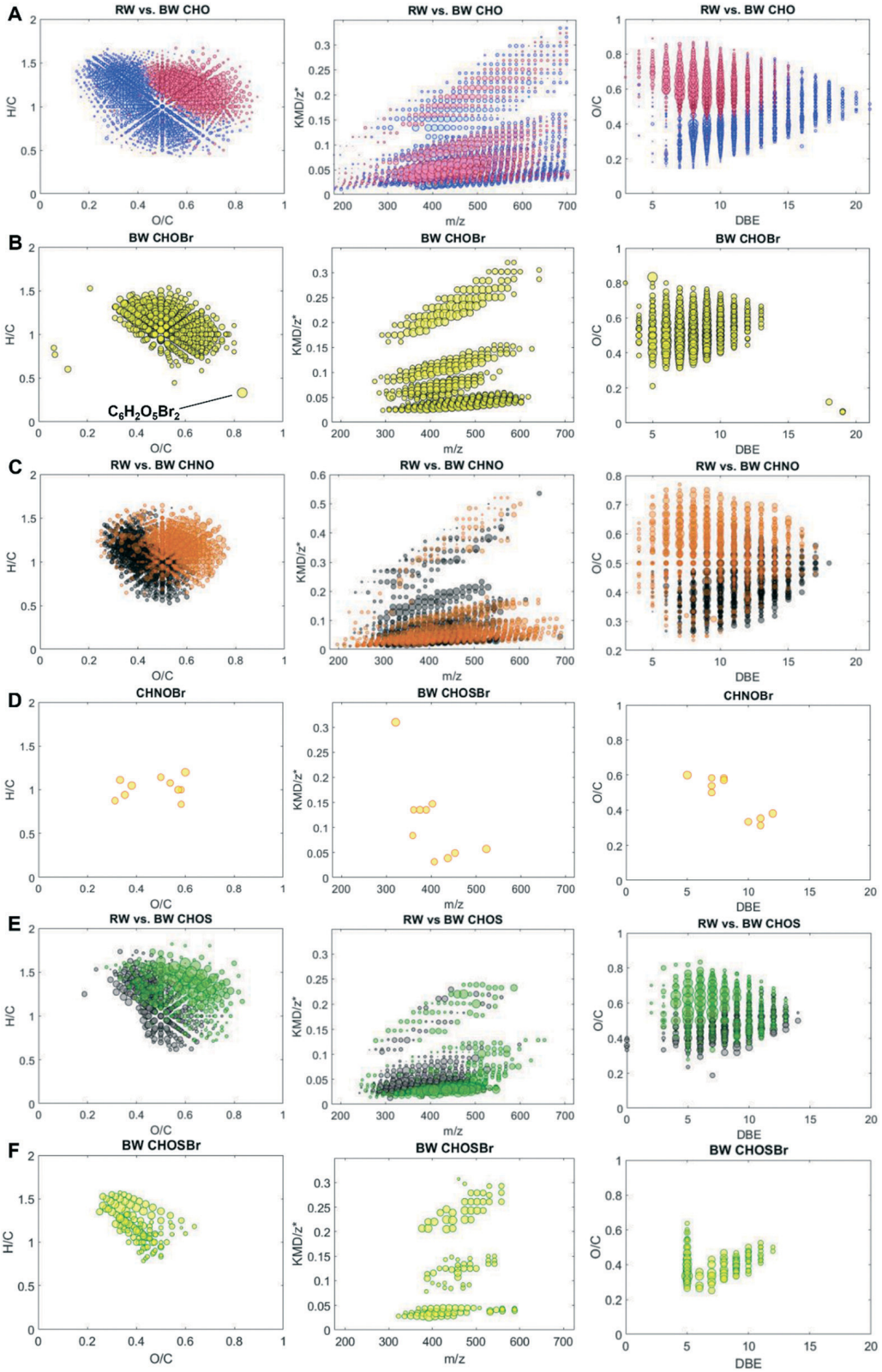

Fig. 2 (left) Hydrogen to carbon ratio (H/C) *versus* oxygen to carbon ratio (O/C), (center) KMD/*z** *versus* exact mass, and (right) O/C *versus* double bond equivalent (DBE) for molecular formula assignments in RW and BW PPL extracts. Bubble size corresponds to relative intensity in each row from to F. (A) A comparison of CHO formula assignments where blue dots are intensities that are relatively decreased from RW and red dots are intensities that are relatively increased in BW. (B) CHOBr formula assignments in BW (yellow dots). (C) A comparison of CHNO formula assignments where black dots are intensities that are relatively decreased from RW and orange dots are intensities that are relatively increased in BW. (D) CHNOBr formula assignments in BW (yellow dots). (E) A comparison of CHOS formula assignments where gray dots are intensities that are relatively decreased from RW and green dots are intensities that are relatively increased in BW. (F) CHOSBr formula assignments in BW (yellow dots). The formula assignment for one highly oxygenated Br-DBP in (B) is noted because this molecular ion was fragmented using Orbitrap MS/MS.

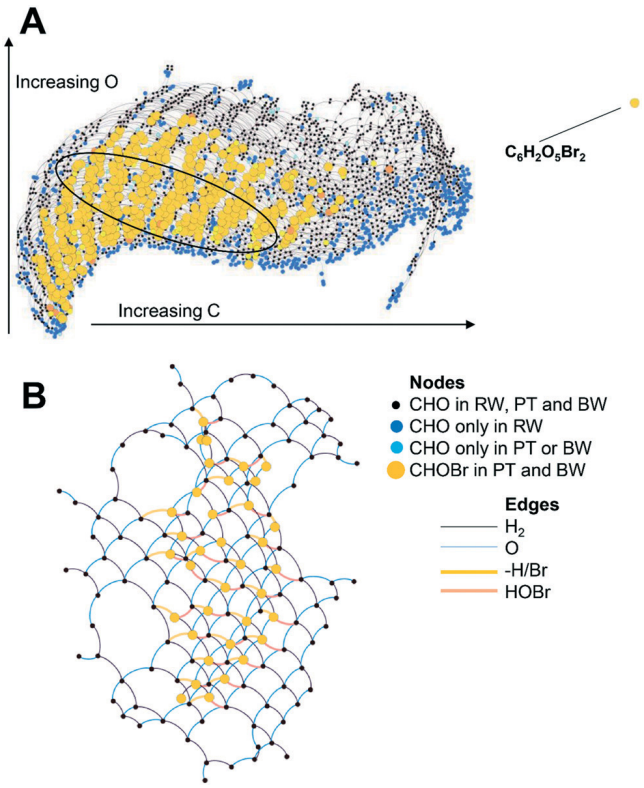

Fig. 3 (A) Mass difference network analysis of all CHO in RW, PT, and BW PPL extracts and CHOBr in PT and BW PPL extracts to show that substitution reactions (H for Br) or addition reactions (HOBr) might explain the formation of Br-DBPs in PT and BW samples. (B) The mass difference network of just $C_{18}HO$ and $C_{18}HOBr$ formulas (highlighted with a black oval in (A)) to more clearly show the edges between molecular formulas.

carboxylic acid (SPC) molecular ions (Fig. 4). Hydroxylation and bromination of suspected SPCs was also visualized with the network analysis (SPC–H/+OH and –H/+Br), suggesting that hydroxylation and bromination are common reactions in this CHOS pool (Fig. 4 and S13†). SPCs are known biodegradation products of LAS,[94] and it is possible that surfactants such as LAS are used in cleaning procedures or are already present in raw water. While this analysis does not confirm the presence of SPC structures and LAS, concentrations should be measured in future work. The intensity patterns in the homologous series of suspected SPC molecular ions and their proposed bromination products are similar, suggesting that these ions are highly related (Fig. 4 and S13†). LAS and SPC molecular ions have been identified in effluent organic matter[95] and a total LAS concentration of 20 μg L^{-1} has been detected in the RO permeate at a desalination plant previously.[96] Thus, the transformation and halogenation of SPCs warrants further study.

The molecular ions of the CHOSBr pool that could not be explained by these reaction mechanisms (Fig. S12†) may be due to the complexity of HOBr reactions with sulfur-containing compounds, and possibly by reaction of surfactant co-products and their degradation products. It also has been demonstrated that reduced sulfur compounds are readily oxidized[27,97] and have a high reactivity for chlorine.[98] In estuarine waters, these reduced sulfur species may present and somewhat stabilized due to their ability to form strong complexes with copper.[99] Previous work has shown that the sulfur containing amino acids cysteine and methionine rapidly react with HOCl.[100] However, the major reaction products of cysteine (a thiol) were disulfides and sulfonic acids and the major reaction product of methionine were sulfoxides.[100] Subsequent work further demonstrated that sulfonic acids are major reaction products formed from the chlorination of reduced sulfur species.[98] CHOS formulas in RW PPL extracts had a Cos_{wt} of −0.17 ± 0.40, suggesting that a large number of CHOS formulas were reduced, and therefore have more complex reaction mechanisms with HOBr (ref. 27) than CHO compounds. Overall, the CHOS pool was more oxidized in BW (higher O/C ratios and lower DBE-O values) relative to RW, suggesting that HOBr reactions oxidize the reduced formulas in CHOS pool but often do not lead to Br incorporation into the CHOS pool. We also did not consider desulfonation during halogenation, which could further complicate the interplay between the CHO and CHOS pools.

While very few molecular formulas were found in ROP and DW WAX extracts, RW, PT, and BW WAX extracts also contained a significant number of molecular ions that were not present in PPL extracts, albeit with overall lower intensities when compared to PPL samples (Fig. S11†). CHO formulas in WAX extracts had a lower center of mass (~365 to 400 Da), higher average O/C_{wt} ratios of (0.73 to 0.77), and lower average H/C_{wt} ratios (0.92 to 0.97) than PPL extracts (Fig. S4 and Table S2†). These formulas are likely made up of highly oxygenated polar compounds such as small organic acids or possibly carboxylated/hydroxylated aromatic glycosides that are not or are only weakly bound by PPL. Because many organic carboxylic acids can have low pK_a values <3,[101] this would explain their charge during extraction at pH 2 and their affinity for the weak anionic exchange cartridge. There were more CHNO formulas found in WAX extracts than CHOS formulas, but both groups occupied the same area in van Krevelen space as CHO compounds (Fig. S4†). Only 20 brominated compounds were found in the BW WAX extract (Table S3†), and some had relatively low mass and high intensity enabling fragmentation studies by Orbitrap MS/MS (described in the next section).

3.3 Targeted analysis of select Br-DBPs by Orbitrap MS/MS

Several candidate molecular ions in both BW PPL and WAX extracts were selected for analysis by Orbitrap MS/MS. One molecular ion in the PPL extract (*m/z* 310.8196 in the FT-ICR-mass spectrum and *m/z* 310.8191 in the Orbitrap mass spectrum) had sufficiently high intensity (Fig. S6†) and a large mass defect to be used for targeted analyses using Orbitrap MS/MS (Table 1). This ion was assigned the neutral

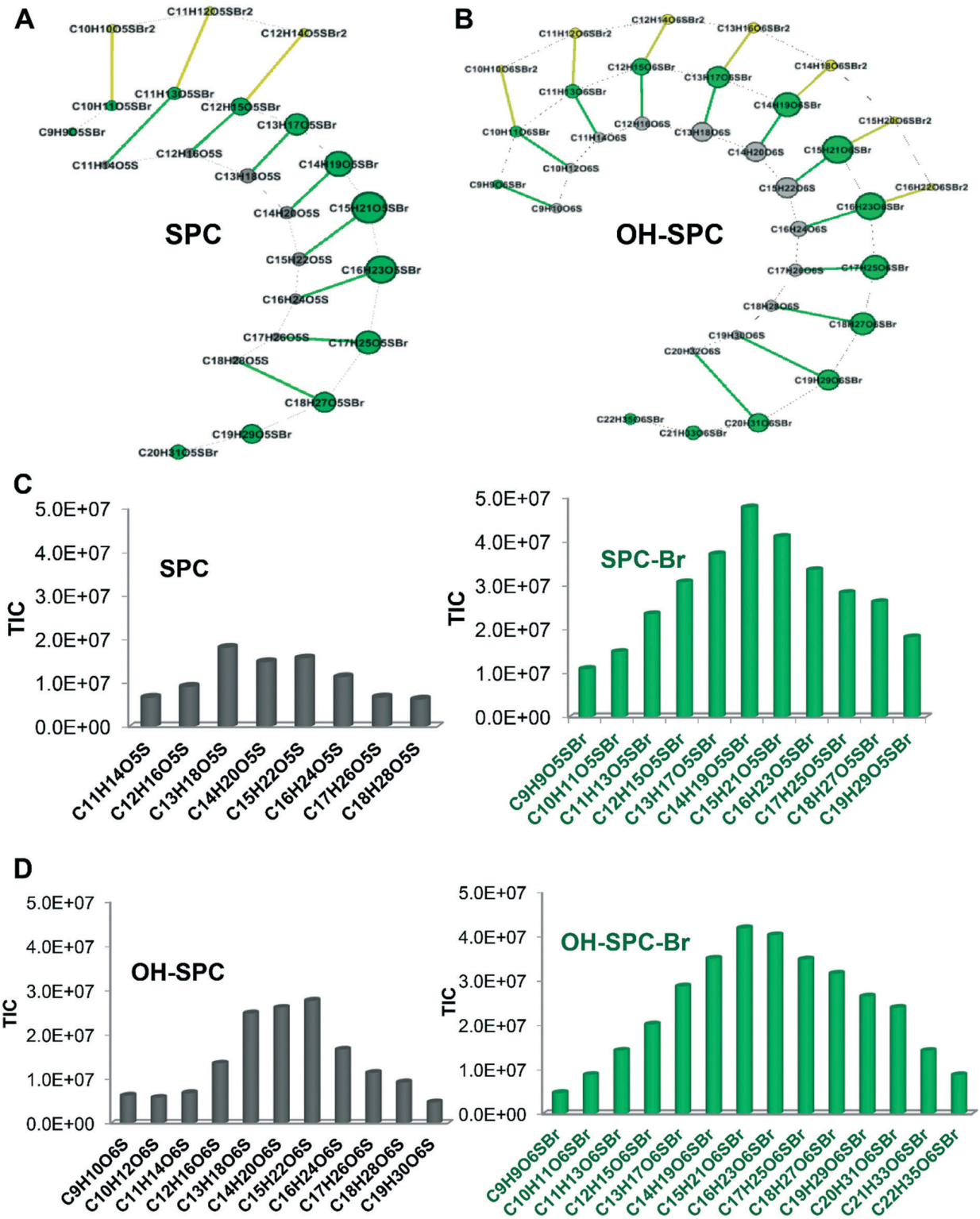

Fig. 4 (A) Mass difference network analysis of all CHOS formulas that match formulas for sulfophenyl carboxylic acids (SPCs) (gray circles) in RW, PT, and BW PPL extracts and CHOSBr formulas (green circles) in PT and BW PPL extracts to see if substitution reactions (H for Br, green lines) might explain the formation of Br-DBPs in PT and BW samples. Yellow lines are also a transition of –H/+Br to $CHOSBr_2$ (yellow circles) molecular formulas (B) mass difference network between CHOS formulas that match hydroxylation (+OH) of the CHOS formulas in (A) and CHOSBr formulas; same colors as (A) apply. (C) Total ion count (TIC) *versus* homologous series (formulas spaced by CH_2) of CHOS formulas (gray, left) and CHOSBr formulas (green, right) in the network displayed in (A). (D) TIC *versus* homologous series (formulas spaced by CH_2) of CHOS formulas (gray, left) and CHOSBr formulas (green, right) in the network displayed in (B).

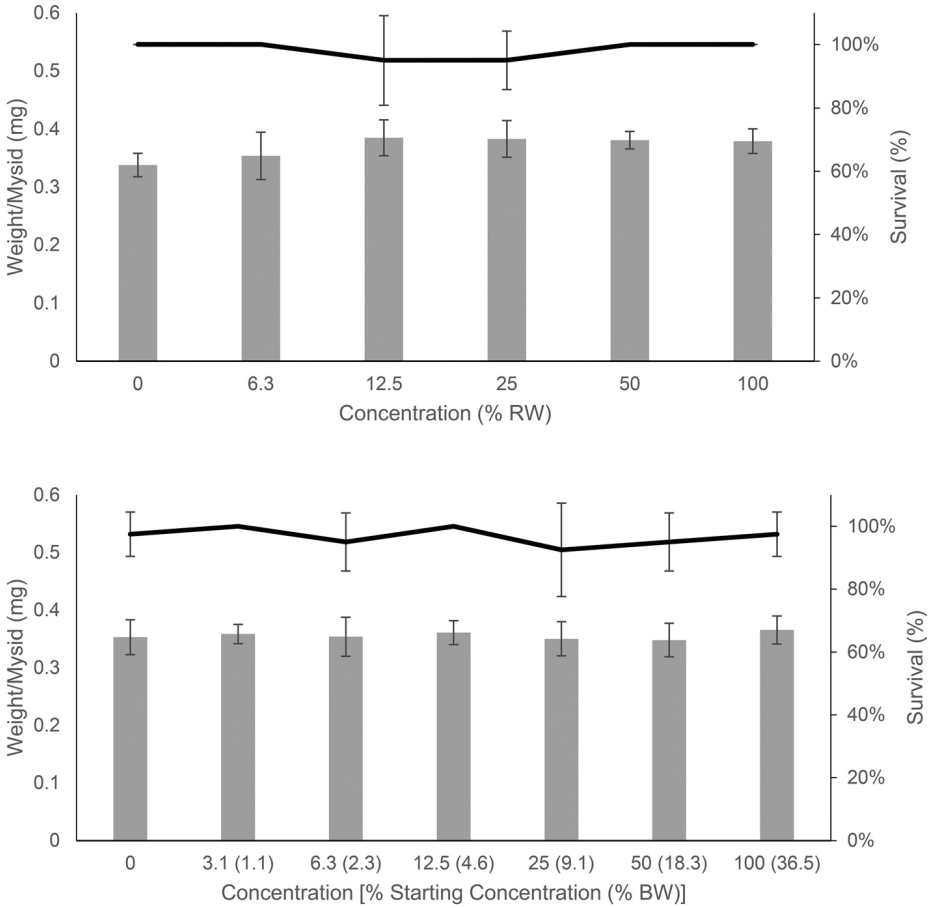

Fig. 5 Average individual weight of mysid shrimp (mg, gray bars, left axis) and percentage survival (%, black line, right axis) at the end of the test (7 days) ± standard deviation *versus* concentration of exposure water for (top) raw water (RW) and (bottom) RO reject water (BW). BW concentrations are given both in percent of starting concentration and overall percent of BW contribution (in parentheses) as BW was initially diluted to match the salinity of RW to avoid salinity-driven toxicity. All test acceptability criteria were met including positive controls (KCl) that were within the range of expected results.

formula of $C_6H_2O_5Br_2$ and is potentially a dibromofuran dicarboxylic acid based on the loss of CO_2 from the molecular ion and from its $^{79}Br^{81}Br$ isotopologue (Table 1). Although additional fragments did not have sufficient intensity to be identified by the SIRIUS 4 software,[72] this compound's precursor ($C_6H_4O_5$) and loss of CO_2 was observed in the RW PPL extract by Orbitrap MS/MS (Table 1).

While 2,5-dibromofuran 3,4-dicarboxylic acid is only a proposed structure for the molecular formula $C_6H_2O_5Br_2$, evidence for halogenated furoic acids has been presented previously.[14] Furans are a class of volatile organic compounds, and very low levels (up to 0.03 ng L^{-1} 3-bromofuran) have been detected in water samples collected from Australian salt lakes and the Dead Sea.[102] Additionally, 2,5-furandicarboxylic acid can be synthesized from a cellulose biomass derivative (5-hydroxylmethylfurfural), and has recently been presented as a substitute for phthalates (derived from fossil fuels) in polyesters.[103] If the production of furandicarboxylic acids increases significantly in the future, these compounds may become far more prevalent in natural waters. Previous work also observed CO_2 losses in MS/MS spectra of two Br-DBPs generated by the reaction of bromine with SRFA.[53] While only based on limited data, perhaps many of the unknown DBPs found here and previously[50,53] that contain carboxyl groups can be analyzed using negative ion-ESI-MS/MS in the future.

One high intensity ion (*m*/*z* 250.8018 in the FT-ICR mass spectrum and *m*/*z* 250.8013 in the Orbitrap mass spectrum) in the BW WAX extract had a neutral molecular formula of $CH_2Br_2SO_3$ and was proposed to be dibromomethanesulfonic acid. Although intensities were much lower than their parent ions, the ^{79}Br fragment was detected from the $CH_2{}^{79}Br_2SO_3$ isotopologue and both the ^{79}Br and ^{81}Br fragments were detected from the $CH_2{}^{79}Br^{81}BrSO_3$ isotopologue (Table 2). Dibromomethanesulfonic acid was also identified as a DBP from the disinfectant 3-bromo-1-chloro-5,5-dimethylhydatoin, which is commonly used in hot tubs.[104] Furthermore, tribromomethanesulfonic acid was suspected to be an abundant molecular ion found in electrochlorinated ballast water using FT-ICR MS.[50] Based on these results, we believe the production of bromomethanesulfonic acids results from chlorination of DOM in the presence of bromide. Recently, halogenated methanesulfonic acids were identified in a variety of samples including surface water, ground water, urban effluent, and drinking water using hydrophilic

Table 1 A possible brominated disinfection byproduct (Br-DBP) in the PPL extract of reject water (1 : 40 dilution in methanol) and its potential precursor in the PPL extract of raw water (1 : 10 dilution in methanol) analyzed by Orbitrap MS/MS. Collision energies ranged from 0 to 40 eV. Bold masses are precursor ions in each experiment; italic masses are fragment ions

Observed ionic mass (neutral mass)	Calculated mass (mass error, ppm)	Neutral formula	Intensity (CID = 0)	Intensity (CID = 10)	Intensity (CID = 20)	Intensity (CID = 30)	Intensity (CID = 40)	Potential Br-DBP
310.8191 (311.8264)	311.8264 (1.7)	$C_6H_2O_5{}^{79}Br_2$	3714	542	0	0	0	2,5-Dibromofuran-3,4-dicarboxylic acid
266.8295 (267.8369)	267.8369 (0.71)	$C_5H_2O_3{}^{79}Br_2$	0	1810	3337	3329	3124	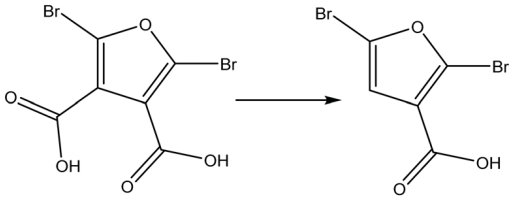
312.8121 (313.8243)	313.8249 (1.8)	$C_6H_2O_5{}^{79}Br^{81}Br$	8124	2277	0	0	0	
268.8273 (269.8346)	269.8346 (1.7)	$C_5H_2O_3{}^{79}Br^{81}Br$	0	4074	6306	6996	6853	
154.9991 (156.0064)	156.0059 (3.2)	$C_6H_4O_5$	2711	1884	0	0	0	3,4-Furandicarboxylic acid
111.0094 (112.0167)	112.0161 (5.6)	$C_5H_4O_3$	0	392	2182	2457	2030	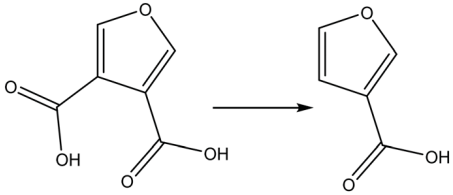

Table 2 Possible brominated disinfection byproducts (Br-DBPs) in the WAX extract of reject water (1 : 3 dilution in methanol) analyzed by Orbitrap MS/MS. Collision energies ranged from 0 to 40 eV. Bold masses are precursor ions in each experiment; italic masses are fragment ions

Observed ionic mass (neutral mass)	Calculated mass (error, ppm)	Neutral formula	Intensity (CID = 0)	Intensity (CID = 10)	Intensity (CID = 20)	Intensity (CID = 30)	Intensity (CID = 40)	Potential Br-DBP
250.8013 (251.8086)	251.8091 (2.2)	$CH_2{}^{79}Br_2SO_3$	613 789	0	0	0	0	Dibromomethanesulfonic acid
78.9188 (–)	78.9183 (0.5)	$^{79}Br^-$	0	0	434	921	959	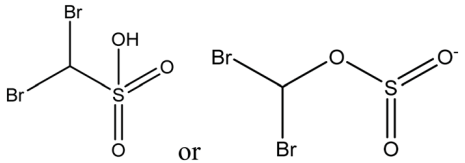
252.7994 (253.8060)	253.8249 (4.4)	$CH_2{}^{79}Br^{81}Br\ SO_3$	115 203	ND	81 117	0	ND	
78.9188 (–)	78.9183 (0.7)	$^{79}Br^-$	0	ND	1083	942	ND	
80.9168 (–)	80.9163 (0.3)	$^{81}Br^-$	0	ND	1693	1533	ND	
293.8396 (294.8469)	294.8480 (2.6)	$C_6H_3NO_3{}^{79}Br_2$	3946.7	425	0	0	ND	4,6-Dibromo-5-hydroxypicolinic acid
249.8496 (250.8568)	250.8581 (0.9)	$C_5H_3NO^{79}Br_2$	0	1480	2078	1919	ND	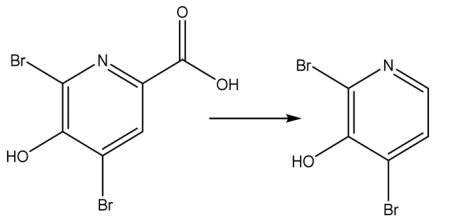
295.8372 (296.8447)	296.8459 (4.4)	$C_6H_3NO_3{}^{79}Br^{81}Br$	6696	1270	0	0	ND	
251.8476 (252.8550)	252.8561 (4.2)	$C_5H_3NO^{79}Br^{81}Br$	0	3269	5159	4481	ND	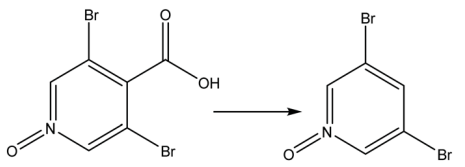
214.8339 (215.842)	215.8422 (0.3)	$C_2H_2O_2{}^{79}Br_2$	3426	0 (CID = 15)	0	0	ND	Dibromoacetic acid
170.8445 (171.8518)	171.8523 (1.5)	$CH_2{}^{79}Br_2$	0	358 (CID = 15)	255	0	ND	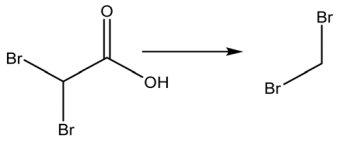

interaction liquid chromatography-HRMS,[105] suggesting that this class of DBPs or pollutants warrants further study to elucidate their toxicity, or lack thereof, and environmental fate.

One dibromo nitrogen-containing molecular ion was evaluated with Orbitrap MS/MS (*m*/*z* 293.8407 in the FT-ICR mass spectrum and *m*/*z* 293.8396 in the Orbitrap mass spectrum) and had a neutral molecular formula of $C_6H_3NO_3Br_2$. Based on the loss of CO_2, this compound is likely a carboxylic acid and could possibly be a brominated hydroxypyridine carboxylic acid (*e.g.* 4,6-dibromo-5-hydroxypicolinic acid). This compound has not been previously identified as a DBP, and there is very little information on halogenated hydroxypicolinic acids. However, niacin or vitamin B3 (a pyridine carboxylic acid) is an essential micronutrient found in marine algae[106] and is widely used, especially for its therapeutic effects likely increasing HDL cholesterol levels.[107] This dibrominated compound's presumed precursor, 5-hydroxypicolinic acid, can be produced by marine microbes like *Nocardia* species.[108] Components of DNA (purine bases and pyrimidines) readily formed DBPs with various levels of genotoxicity,[109] thus an investigation of DBP formation from pyridine derivatives is warranted. Another small dibrominated molecular ion with the neutral molecular formula $C_2H_2O_2Br_2$ was presumed to be dibromoacetic acid, a known DBP with a parent ion at *m*/*z* 214.8339 and a fragment ion at *m*/*z* 170.8445 (Table 2). Although the concentrations of dibromoacetic acid were not determined for our samples, haloacetic acids could be abundant DBPs.[32,110] This compound and other haloacetic acids have known genotoxic activity.[2,8,111] However, BW did not show any acute or chronic toxicity (as assessed by mortality and growth differences) to mysid shrimp (described below), but this assessment was based on a direct comparison between raw water and BW.

3.4 Toxicity of reject water

Despite the identification of 519 Br-DBPs in reject water PPL and WAX extracts including one compound with known toxicity (dibromoacetic acid), BW did not show any toxicity to mysid shrimp after a 7 day exposure. In fact, neither RW nor the BW showed a significant response for growth or survival (Fig. 5 top and bottom, respectively). Individual chemicals and any combined toxicity of the multiple chemicals in the RW and BW collected at that time were below toxicity thresholds for the mysid shrimp. However, it should be noted that the original salinity of the BW was 60 and that BW toxicity tests began at a concentration of 36.5% instead of 100% (*i.e.* neat stock solution with no dilution) in order to avoid salinity-driven toxicity. For toxicity tests mysid shrimp can be used at a range of salinities as they are typically in conditions of S = 15 to 30. A study by Pillard *et al.*[81] demonstrated significant mortality (at only 48 hours) in mysid shrimp to artificial seawater above salinity 45, which suggests that exposing mysid shrimp to 100% BW would have led to significant negative impacts irrespective of the chemical contaminants present. Similarly, exposures of mysids to hypersaline brine resulted in NOECs of survival and growth between salinity 44.9–45.8 and salinity 49.2–50.2, respectively.[62] Therefore, as our objective was not to address the effects of higher salinity but the toxic effects of contaminants of concern, the initial salinity of the BW was adjusted to 22.5 (*i.e.* a 2.74-fold dilution or a starting % of the effluent at 36.5%; see Fig. 5 and Table S4†) to be within the EPA test guidelines and to match the salinity of the RW (Table S5†).

Toxicity endpoints of LC50s, and IC25s were >100% and NOECs were 100% for both RW and BW (see Table S6†) demonstrating no significant toxicity of either test waters. This data is similar to previous studies with brine/effluents from desalination plants. For example, Bodensteiner *et al.*[61] found no significant impact of the brine water [which is blended with waste water treatment plant (WWTP) effluent before release] to a number of marine species, and interestingly this water actually reduced the toxicity of the WWTP effluent. This study reported in mysid shrimp survival LC/IC50s of >100% and NOEC of 100% effluent and growth LC50 at >100% and a NOEC of 75% effluent (*i.e.* using unadjusted brine at S = 47 and adjusted brine at S = 30). Although it should be noted that where reject waters are discharged there are many different local resident species that may be more or less sensitive than standard EPA test organisms (*i.e.* reflective of the species, life-stage and/or duration of the test). However, the RW showed an interesting non-significant response for growth with larger organisms (*i.e.* increased growth) in the higher concentrations compared to controls of influent suggesting this natural seawater provides something to the mysids that is not provided in the artificial seawater used for the controls and dilution water. As mentioned earlier all test acceptability criteria were met. For example, the calculated 7 day IC_{25} for the positive control (KCl) was 0.45 g L^{-1} (95% confidence interval: 0.44 to 0.51 g L^{-1}) which is slightly lower than the reported values of approximately 0.93 to 0.95 g L^{-1} by Pillard *et al.*[80] However, if the 96 h LC_{50} is calculated from these data, it is calculated at 0.53 g L^{-1} (95% CI: 0.49 to 0.55 g L^{-1}) which is very similar to results from Garcia *et al.*,[79] which calculated a 96 h LC_{50} at 0.501 g L^{-1}.

4 Conclusions

Our results reveal substantial changes in water optical properties and molecular complexity during the desalination process. Organic bromine concentrations were below detection in drinking water, but chlorination produced substantial changes in RO reject water. These included changes in optical properties (absorbance and fluorescence spectra), increases OrganoBr concentrations, and the production of hundreds of Br-DBPs. Network analysis of CHO and CHOBr formulas suggests that substitution reactions are a likely mechanism of bromine incorporation into DOM, as suggested in previous studies.[31,52,54,57] Thus, increases in

absorbance spectral slopes, decreases in SUVA values, and increases in fluorescence apparent quantum yield spectra may be attributed to bromine substitution on aromatic molecules and not necessarily due to their loss (*e.g.* ring cleavage). There were several sulfur-containing Br-DBPs identified in RO reject water, and a group of these molecular ions could be due to the bromination of sulfophenyl carboxylic acids. However, some CHOSBr ions could not be explained by substitution or addition reactions. Given that sulfur can exist in a variety of oxidation states and the sulfur pool within DOM can undergo a variety of transformations in surface waters,[112] it is not surprising that the formation of CHOSBr formulas cannot be predicted by substitution and addition reactions alone.

Based on Orbitrap MS/MS experiments, halogenated furoic acids/furandicarboxylic acids and halogenated pyridine carboxylic acids may warrant further investigation as new classes of DBPs. However, all samples analyzed were SPE extracts and perhaps polar carboxylic acids preferentially ionize using negative ion-ESI. Based on these limited data and caveats, it is uncertain whether the majority of Br-DBPs found here have carboxylic acid functional groups. Nonetheless, >500 Br-containing formulas were identified in RO reject water, highlighting that many Br-DBPs have yet to be identified. Additional exploration of the DOM and DBP pool could involve using positive ion-ESI and different SPE techniques. These non-targeted and qualitative approaches may give a more holistic view of the Br-DBPs generated from seawater desalination and inform targeted research efforts.

Despite the number of Br-containing DBPs identified here, their environmental fate still needs to be addressed. Based on our encouraging toxicity results, 2.74-fold diluted BW water did not limit growth or decrease survival of mysid shrimp. There is the potential for longer term chronic impacts and impacts to other sublethal endpoints (*e.g.* genetic damage, endocrine disruption). It is also possible that biological transformations and abiotic reactions (*e.g.* photochemical reactions) will degrade these DBPs or transform them into compounds with unknown reactivity in the environment. Thus, tracking the changes in molecular composition of BW during bio- and photo-degradation experiments is a crucial next step in furthering our understanding of DBP environmental fate.

Conflicts of interest

The authors declare no conflicts of interest.

Acknowledgements

We thank the desalination plant for their willingness to participate in this project and their support and assistance in collecting samples. We are grateful to two reviewers for their constructive comments that greatly improved this manuscript. This work was supported by National Science Foundation Environmental Chemical Sciences Grants 1708766 and 1708461 (to Michael Gonsior and Susan Richardson, respectively). This is contribution 5875 and Ref. No. [UMCES] CBL 2020-139 of the University of Maryland Center for Environmental Science.

References

1 J. J. Rook, Formation of haloforms during chlorination of natural waters, in *Water Treatment and Examination*, 23rd edn, 1974, pp. 234–243.
2 S. D. Richardson, M. J. Plewa, E. D. Wagner, R. Schoeny and D. M. DeMarini, Occurrence, genotoxicity, and carcinogenicity of regulated and emerging disinfection by-products in drinking water: A review and roadmap for research, *Mutat. Res., Rev. Mutat. Res.*, 2007, **636**, 178–242.
3 S. D. Richardson and C. Postigo, Drinking Water Disinfection By-products, in *Emerging Organic Contaminants and Human Health*, ed. D. Barceló, Springer Berlin Heidelberg, Berlin, Heidelberg, 2012, pp. 93–137.
4 K. P. Cantor, Drinking water and cancer, *Cancer Causes Control*, 1997, **8**, 292–308.
5 C. M. Villanueva, K. P. Cantor, S. Cordier, J. J. K. Jaakkola, W. D. King, C. F. Lynch, S. Porru and M. Kogevinas, Disinfection byproducts and bladder cancer: A pooled analysis, *Epidemiology*, 2004, **15**, 357–367.
6 K. P. Cantor, Carcinogens in Drinking Water: The Epidemiologie Evidence, *Rev. Environ. Health*, 2010, **25**, 9–16.
7 X. F. Li and W. A. Mitch, Drinking Water Disinfection Byproducts (DBPs) and Human Health Effects: Multidisciplinary Challenges and Opportunities, *Environ. Sci. Technol.*, 2018, **52**, 1681–1689.
8 E. D. Wagner and M. J. Plewa, CHO cell cytotoxicity and genotoxicity analyses of disinfection by-products: An updated review, *J. Environ. Sci.*, 2017, **58**, 64–76.
9 F. Qin, Y. Y. Zhao, Y. Zhao, J. M. Boyd, W. Zhou and X. F. Li, A toxic disinfection by-product, 2,6-dichloro-1,4-benzoquinone, identified in drinking water, *Angew. Chem., Int. Ed.*, 2010, **49**, 790–792.
10 Y. Pan and X. Zhang, Four groups of new aromatic halogenated disinfection byproducts: Effect of bromide concentration on their formation and speciation in chlorinated drinking water, *Environ. Sci. Technol.*, 2013, **47**, 1265–1273.
11 G. Ding, X. Zhang, M. Yang and Y. Pan, Formation of new brominated disinfection byproducts during chlorination of saline sewage effluents, *Water Res.*, 2013, **47**, 2710–2718.
12 C. H. Jeong, E. D. Wagner, V. R. Siebert, S. Anduri, S. D. Richardson, E. J. Daiber, A. B. McKague, M. Kogevinas, C. M. Villanueva, E. H. Goslan, W. Luo, L. M. Isabelle, J. F. Pankow, R. Grazuleviciene, S. Cordier, S. C. Edwards, E. Righi, M. J. Nieuwenhuijsen and M. J. Plewa, Occurrence and toxicity of disinfection byproducts in European drinking waters in relation with the HIWATE epidemiology study, *Environ. Sci. Technol.*, 2012, **46**, 12120–12128.

13 Y. Zhao, J. Anichina, X. Lu, R. J. Bull, S. W. Krasner, S. E. Hrudey and X. F. Li, Occurrence and formation of chloro- and bromo-benzoquinones during drinking water disinfection, *Water Res.*, 2012, **46**, 4351–4360.
14 M. Gonsior, P. Schmitt-Kopplin, H. Stavklint, S. D. Richardson, N. Hertkorn and D. Bastviken, Changes in Dissolved Organic Matter during the Treatment Processes of a Drinking Water Plant in Sweden and Formation of Previously Unknown Disinfection Byproducts, *Environ. Sci. Technol.*, 2014, **48**, 12714–12722.
15 C. Postigo, C. I. Cojocariu, S. D. Richardson, P. J. Silcock and D. Barcelo, Erratum to: Characterization of iodinated disinfection by-products in chlorinated and chloraminated waters using Orbitrap based gas chromatography-mass spectrometry, *Anal. Bioanal. Chem.*, 2016, **408**, 6869–6870.
16 C. Postigo, S. D. Richardson and D. Barceló, Formation of iodo-trihalomethanes, iodo-haloacetic acids, and haloacetaldehydes during chlorination and chloramination of iodine containing waters in laboratory controlled reactions, *J. Environ. Sci.*, 2017, **58**, 127–134.
17 C. Postigo, D. M. Demarini, M. D. Armstrong, H. K. Liberatore, K. Lamann, S. Y. Kimura, A. A. Cuthbertson, S. H. Warren, S. D. Richardson, T. McDonald, Y. M. Sey, N. O. B. Ackerson, S. E. Duirk and J. E. Simmons, Chlorination of Source Water Containing Iodinated X-ray Contrast Media: Mutagenicity and Identification of New Iodinated Disinfection Byproducts, *Environ. Sci. Technol.*, 2018, **52**, 13047–13056.
18 J. L. Luek, P. Schmitt-Kopplin, P. J. Mouser, W. T. Petty, S. D. Richardson and M. Gonsior, Halogenated Organic Compounds Identified in Hydraulic Fracturing Wastewaters Using Ultrahigh Resolution Mass Spectrometry, *Environ. Sci. Technol.*, 2017, **51**, 5377–5385.
19 H. K. Liberatore, M. J. Plewa, E. D. Wagner, J. M. Vanbriesen, D. B. Burnett, L. H. Cizmas and S. D. Richardson, Identification and Comparative Mammalian Cell Cytotoxicity of New Iodo-Phenolic Disinfection Byproducts in Chloraminated Oil and Gas Wastewaters, *Environ. Sci. Technol. Lett.*, 2017, **4**, 475–480.
20 D. Zahn, R. Meusinger, T. Frömel and T. P. Knepper, Halomethanesulfonic acids - a new class of polar disinfection byproducts: Standard synthesis, occurrence, and indirect assessment of mitigation options, *Environ. Sci. Technol.*, 2019, **53**, 8994–9002.
21 G. Huang, P. Jiang, L. K. Jmaiff Blackstock, D. Tian and X. F. Li, Formation and Occurrence of Iodinated Tyrosyl Dipeptides in Disinfected Drinking Water, *Environ. Sci. Technol.*, 2018, **52**, 4218–4226.
22 G. Huang, L. K. Jmaiff Blackstock, P. Jiang, Z. Liu, X. Lu and X. F. Li, Formation, Identification, and Occurrence of New Bromo- and Mixed Halo-Tyrosyl Dipeptides in Chloraminated Water, *Environ. Sci. Technol.*, 2019, **53**, 3672–3680.
23 D. Zhang, W. Chu, Y. Yu, S. W. Krasner, Y. Pan, J. Shi, D. Yin and N. Gao, Occurrence and Stability of Chlorophenylacetonitriles: A New Class of Nitrogenous Aromatic DBPs in Chlorinated and Chloraminated Drinking Waters, *Environ. Sci. Technol. Lett.*, 2018, **5**, 394–399.
24 S. Yu, T. Lin, W. Chen and H. Tao, The toxicity of a new disinfection by-product, 2,2-dichloroacetamide (DCAcAm), on adult zebrafish (Danio rerio) and its occurrence in the chlorinated drinking water, *Chemosphere*, 2015, **139**, 40–46.
25 D. Kim, G. L. Amy and T. Karan, Disinfection by-product formation during seawater desalination: A review, *Water Res.*, 2015, **81**, 343–355.
26 E. Agus, N. Voutchkov and D. L. Sedlak, Disinfection by-products and their potential impact on the quality of water produced by desalination systems: A literature review, *Desalination*, 2009, **237**, 214–237.
27 M. Deborde and U. von Gunten, Reactions of chlorine with inorganic and organic compounds during water treatment-Kinetics and mechanisms: A critical review, *Water Res.*, 2008, **42**, 13–51.
28 B. Heeb, J. Criquet, S. G. Zimmermann-Steffens and U. von Gunten, Oxidative treatment of bromide-containing waters: Formation of bromine and its reactions with inorganic and organic compounds - A critical review, *Water Res.*, 2013, **48**, 15–42.
29 K. Ito, R. Nomura, T. Fujii, M. Tanaka, T. Tsumura, H. Shibata and T. Hirokawa, Determination of nitrite, nitrate, bromide, and iodide in seawater by ion chromatography with UV detection using dilauryldimethylammonium-coated monolithic ODS columns and sodium chloride as an eluent, *Anal. Bioanal. Chem.*, 2012, **404**, 2513–2517.
30 F. J. Millero, R. Feistel, D. G. Wright and T. J. McDougall, The composition of Standard Seawater and the definition of the Reference-Composition Salinity Scale, *Deep Sea Res., Part I*, 2008, **55**, 50–72.
31 E. E. Lavonen, M. Gonsior, L. J. Tranvik, P. Schmitt-Kopplin and S. J. Köhler, Selective chlorination of natural organic matter: Identification of previously unknown disinfection byproducts, *Environ. Sci. Technol.*, 2013, **47**, 2264–2271.
32 J. Le Roux, N. Nada, M. T. Khan and J. P. Croué, Tracing disinfection byproducts in full-scale desalination plants, *Desalination*, 2015, **359**, 141–148.
33 E. G. Brown Jr., J. Laird and M. Cowin, *California Water Plan Update 2013*, State of California, 2013, vol. 2013.
34 O. of W. (4605M) E. 816-R-07-007, *National Primary Drinking Water Regulations: The Stage 2 Disinfectants and Disinfection Byproducts Rule (Stage 2 DBPR) Implementation Guidance*, 2007.
35 L. J. Falkenberg and C. A. Styan, The use of simulated whole effluents in toxicity assessments: A review of case studies from reverse osmosis desalination plants, *Desalination*, 2015, **368**, 3–9.
36 J. A. Hawkes, C. Patriarca, P. J. R. Sjöberg, L. J. Tranvik and J. Bergquist, Extreme isomeric complexity of dissolved organic matter found across aquatic environments, *Limnol. Oceanogr. Lett.*, 2018, **3**, 21–30.
37 M. Zark and T. Dittmar, Universal molecular structures in natural dissolved organic matter, *Nat. Commun.*, 2018, **9**, 1–8.

38 E. J. Rochelle-Newall and T. R. Fisher, Chromophoric dissolved organic matter and dissolved organic carbon in Chesapeake Bay, *Mar. Chem.*, 2002, **77**, 23–41.
39 C. Romera-Castillo, H. Sarmento, X. Anton Alvarez-Salgado, J. M. Gasol and C. Marrase, Production of chromophoric dissolved organic matter by marine phytoplankton, *Limnol. Oceanogr.*, 2010, **55**, 1466–1466.
40 D. J. Burdige and J. Homstead, Fluxes of dissolved organic carbon from Chesapeake Bay sediments, *Geochim. Cosmochim. Acta*, 1994, **58**, 3407–3424.
41 J. E. Bauer, W.-J. Cai, P. A. Raymond, T. S. Bianchi, C. S. Hopkinson and P. A. G. Regnier, The changing carbon cycle of the coastal ocean, *Nature*, 2013, **504**, 61–70.
42 J. J. Walsh, Importance of continental margins in the marine biochemical cycling of carbon and nitrogen, *Nature*, 1991, **350**, 53–55.
43 P. A. Raymond and R. G. M. Spencer, Riverine DOM, in *Biogeochemistry of Marine Dissolved Organic Matter*, ed. D. A. Hansell and C. A. Carlson, Academic Press, Burlington, 2015, pp. 509–533.
44 R. Benner and K. Kaiser, Biological and photochemical transformations of amino acids and lignin phenols in riverine dissolved organic matter, *Biogeochemistry*, 2011, **102**, 209–222.
45 M. A. Moran, W. M. Sheldon and R. G. Zepp, Carbon loss and optical property changes during long-term photochemical and biological degradation of estuarine dissolved organic matter, *Limnol. Oceanogr.*, 2000, **45**, 1254–1264.
46 C. G. Fichot and R. Benner, The fate of terrigenous dissolved organic carbon in a river-influenced ocean margin, *Global Biogeochem. Cycles*, 2014, **28**, 300–318.
47 T. Dittmar, K. Whitehead, E. C. Minor and B. P. Koch, Tracing terrigenous dissolved organic matter and its photochemical decay in the ocean by using liquid chromatography/mass spectrometry, *Mar. Chem.*, 2007, **107**, 378–387.
48 M. Gonsior, B. M. Peake, W. T. Cooper, D. Podgorski, J. D. Andrilli and W. J. Cooper, Photochemically induced changes in dissolved organic matter identified by ultrahigh resolution fourier transform ion cyclotron resonance mass spectrometry, *Environ. Sci. Technol.*, 2009, **43**, 698–703.
49 T. Gong, X. Zhang, Y. Li and Q. Xian, Formation and toxicity of halogenated disinfection byproducts resulting from linear alkylbenzene sulfonates, *Chemosphere*, 2016, **149**, 70–75.
50 M. Gonsior, C. Mitchelmore, A. Heyes, M. Harir, S. D. Richardson, W. T. Petty, D. A. Wright and P. Schmitt-Kopplin, Bromination of Marine Dissolved Organic Matter following Full Scale Electrochemical Ballast Water Disinfection, *Environ. Sci. Technol.*, 2015, **49**, 9048–9055.
51 J. Hollender, E. L. Schymanski, H. Singer and P. L. Ferguson, Non-target screening with high resolution mass spectrometry in the environment: Ready to go?, *Environ. Sci. Technol.*, 2017, **51**, 11505–11512.
52 E. E. Lavonen, D. N. Kothawala, L. J. Tranvik, M. Gonsior, P. Schmitt-Kopplin and S. J. Köhler, Tracking changes in the optical properties and molecular composition of dissolved organic matter during drinking water production, *Water Res.*, 2015, **85**, 286–294.
53 H. Zhang, Y. Zhang, Q. Shi, H. Zheng and M. Yang, Characterization of unknown brominated disinfection byproducts during chlorination using ultrahigh resolution mass spectrometry, *Environ. Sci. Technol.*, 2014, **48**, 3112–3119.
54 J. Wenk, M. Aeschbacher, E. Salhi, S. Canonica, U. Von Gunten and M. Sander, Chemical oxidation of dissolved organic matter by chlorine dioxide, chlorine, and ozone: Effects on its optical and antioxidant properties, *Environ. Sci. Technol.*, 2013, **47**, 11147–11156.
55 M. Gonsior, L. C. Powers, E. Williams, A. Place, F. Chen, A. Ruf, N. Hertkorn and P. Schmitt-Kopplin, The chemodiversity of algal dissolved organic matter from lysed Microcystis aeruginosa cells and its ability to form disinfection by-products during chlorination, *Water Res.*, 2019, **155**, 300–309.
56 D. S. Kosyakov, N. V. Ul'yanovskii, M. S. Popov, T. B. Latkin and A. T. Lebedev, Halogenated fatty amides – A brand new class of disinfection by-products, *Water Res.*, 2017, **127**, 183–190.
57 P. Westerhoff, P. Chao and H. Mash, Reactivity of natural organic matter with aqueous chlorine and bromine, *Water Res.*, 2004, **38**, 1502–1513.
58 S. Lattemann and T. Höpner, Environmental impact and impact assessment of seawater desalination, *Desalination*, 2008, **220**, 1–15.
59 R. Miri and A. Chouikhi, Ecotoxicological marine impacts from seawater desalination plants. Desalination, *Desalination*, 2005, **182**, 403–410.
60 J. J. Sadhwani, J. M. Veza and C. Santana, Case studies on environmental impact of seawater desalination, *Desalination*, 2005, **185**, 1–8.
61 S. Bodensteiner, M. Zinkl, J. McCloskey, S. Brander, L. Grabow and P. Sellier, Effects of Desalination Brine Waste Blended with Treated Wastewater in the Aquatic Environment of San Francisco Bay, *Water Practice*, 2008, **2**, 1–9.
62 J. P. Voorhees, B. M. Phillips, B. S. Anderson, K. Siegler, S. Katz, L. Jennings, R. S. Tjeerdema, J. Jensen and M. De La Paz Carpio-Obeso, Hypersalinity toxicity thresholds for nine California ocean plan toxicity test protocols, *Arch. Environ. Contam. Toxicol.*, 2013, **65**, 665–670.
63 L. Weinrich, M. Lechevallier and C. N. Haas, Contribution of assimilable organic carbon to biological fouling in seawater reverse osmosis membrane treatment, *Water Res.*, 2016, **101**, 203–213.
64 R. G. Zepp, W. M. Sheldon and M. A. Moran, Dissolved organic fluorophores in southeastern US coastal waters: correction method for eliminating Rayleigh and Raman scattering peaks in excitation–emission matrices, *Mar. Chem.*, 2004, **89**, 15–36.
65 T. Dittmar, B. Koch, N. Hertkorn and G. Kattner, A simple and efficient method for the solid-phase extraction of dissolved organic matter (SPE-DOM) from seawater, *Limnol. Oceanogr.: Methods*, 2008, **6**, 230–235.

66 S. A. Timko, A. Maydanov, S. L. Pittelli, M. H. Conte, W. J. Cooper, B. P. Koch, P. Schmitt-Kopplin and M. Gonsior, Depth-dependent photodegradation of marine dissolved organic matter, *Front. Mar. Sci.*, 2015, **2**, 1–13.

67 P. Herzsprung, N. Hertkorn, W. Von Tümpling, M. Harir, K. Friese and P. Schmitt-Kopplin, Molecular formula assignment for dissolved organic matter (DOM) using high-field FT-ICR-MS: Chemical perspective and validation of sulphur-rich organic components (CHOS) in pit lake samples, *Anal. Bioanal. Chem.*, 2016, **408**, 2461–2469.

68 P. Herzsprung, N. Hertkorn, W. von Tümpling, M. Harir, K. Friese and P. Schmitt-Kopplin, Understanding molecular formula assignment of Fourier transform ion cyclotron resonance mass spectrometry data of natural organic matter from a chemical point of view, *Anal. Bioanal. Chem.*, 2014, **406**, 7977–7987.

69 J. H. Kroll, N. M. Donahue, J. L. Jimenez, S. H. Kessler, M. R. Canagaratna, K. R. Wilson, K. E. Altieri, L. R. Mazzoleni, A. S. Wozniak, H. Bluhm, E. R. Mysak, J. D. Smith, C. E. Kolb and D. R. Worsnop, Carbon oxidation state as a metric for describing the chemistry of atmospheric organic aerosol, *Nat. Chem.*, 2011, **3**, 133–139.

70 M. M. Yassine, M. Harir, E. Dabek-Zlotorzynska and P. Schmitt-Kopplin, Structural characterization of organic aerosol using Fourier transform ion cyclotron resonance mass spectrometry: aromaticity equivalent approach, *Rapid Commun. Mass Spectrom.*, 2014, **28**, 2445–2454.

71 B. P. Koch and T. Dittmar, Erratum: From mass to structure: An aromaticity index for high-resolution mass data of natural organic matter, *Rapid Commun. Mass Spectrom.*, 2016, **30**, 250.

72 K. Dührkop, M. Fleischauer, M. Ludwig, A. A. Aksenov, A. V. Melnik, M. Meusel, P. C. Dorrestein, J. Rousu and S. Böcker, SIRIUS 4: a rapid tool for turning tandem mass spectra into metabolite structure information, Nat, *Methods*, 2019, **16**, 299–302.

73 D. W. van Krevelen, Graphical-statistical method for the study of structure and reaction processes of coal, *Fuel*, 1950, **29**, 269–284.

74 S. Shakeri Yekta, M. Gonsior, P. Schmitt-Kopplin and B. H. Svensson, Characterization of Dissolved Organic Matter in Full Scale Continuous Stirred Tank Biogas Reactors Using Ultrahigh Resolution Mass Spectrometry: A Qualitative Overview, *Environ. Sci. Technol.*, 2012, **46**, 12711–12719.

75 E. Kendrick, A Mass Scale Based on CH2 = 14.0000 for High Resolution Mass Spectrometry of Organic Compounds, *Anal. Chem.*, 1963, **35**, 2146–2154.

76 A. C. Stenson, A. G. Marshall and W. T. Cooper, Exact Masses and Chemical Formulas of Individual Suwannee River Fulvic Acids from Ultrahigh Resolution Electrospray Ionization Fourier Transform Ion Cyclotron Resonance Mass Spectrometry, *Anal. Chem.*, 2003, **75**, 1275–1284.

77 D. Tziotis, N. Hertkorn and P. Schmitt-Kopplin, Kendrick-analogous network visualisation of ion cyclotron resonance Fourier transform mass spectra: improved options for the assignment of elemental compositions and the classification of organic molecular complexity, *Eur. J. Mass Spectrom.*, 2011, **17**, 415.

78 U.S. Environmental Protection Agency, *Short-term Methods for Estimating the Chronic Toxicity of Effluents and Receiving Waters to Marine and Estuarine Organisms*, EPA/821/R/02/014, 2002, pp. 1–486.

79 K. Garcia, J. B. R. Agard and A. Mohammed, Comparative sensitivity of a tropical mysid Metamysidopsis insularis and the temperate species Americamysis bahia to six toxicants, *Toxicol. Environ. Chem.*, 2008, **90**, 779–785.

80 D. A. Pillard, D. L. DuFresne, J. E. Tietge and D. Caudle, *Development of Salinity Toxicity Relationships for Produced Water Discharges to the Marine Environment*, Final Report, GRI-97/0168, ENSR Consult. and Engl, Fort Collins, CO, 1998.

81 D. A. Pillard, D. L. DuFresne, J. E. Tietge and J. M. Evans, Response of mysid shrimp (Mysidopsis bahia), sheepshead minnow (Cyprinodon variegatus), and inland silverside minnow (Menidia beryllina) to changes in artificial seawater salinity, *Environ. Toxicol. Chem.*, 1999, **18**, 430–435.

82 D. A. Pillard, D. L. DuFresne and M. C. Mickley, Development and Validation of Models Predicting the Toxicity of Major Seawater Ions To the Mysid Shrimp, Americamysis Bahia, *Environ. Toxicol. Chem.*, 2002, **21**, 2131.

83 R. P. Buck, S. Singhadeja and L. B. Rogers, Ultraviolet Absorption Spectra of Some Inorganic Ions in Aqueous Solutions, *Anal. Chem.*, 1954, **26**, 1240–1242.

84 P. Kowalczuk, W. J. Cooper, M. J. Durako, A. E. Kahn, M. Gonsior and H. Young, Characterization of dissolved organic matter fluorescence in the South Atlantic Bight with use of PARAFAC model: Relationships between fluorescence and its components, absorption coefficients and organic carbon concentrations, *Mar. Chem.*, 2010, **118**, 22–36.

85 J. R. Helms, A. Stubbins, J. D. Ritchie, E. C. Minor, D. J. Kieber and K. Mopper, Absorption spectral slopes and slope ratios as indicators of molecular weight, source, and photobleaching of chromophoric dissolved organic matter, *Limnol. Oceanogr.*, 2008, **53**, 955–969.

86 J. L. Weishaar, G. R. Aiken, B. A. Bergamaschi, M. S. Fram, R. Fujii and K. Mopper, Evaluation of specific ultraviolet absorbance as an indicator of the chemical composition and reactivity of dissolved organic carbon, *Environ. Sci. Technol.*, 2003, **37**, 4702–4708.

87 R. Jaffé, K. M. Cawley and Y. Yamashita, Applications of Excitation Emission Matrix Fluorescence with Parallel Factor Analysis (EEM-PARAFAC) in Assessing Environmental Dynamics of Natural Dissolved Organic Matter (DOM) in Aquatic Environments: A Review, in *Advances in the Physicochemical Characterization of Dissolved Organic Matter: Impact on Natural and Engineered Systems*, American Chemical Society, 2014, vol. 1160, pp. 3–27.

88 R. Del Vecchio and N. V. Blough, Photobleaching of chromophoric dissolved organic matter in natural waters: kinetics and modeling, *Mar. Chem.*, 2002, **78**, 231–253.

89 C. M. Sharpless and N. V. Blough, The importance of charge-transfer interactions in determining chromophoric dissolved organic matter (CDOM) optical and photochemical properties, *Environ. Sci.: Processes Impacts*, 2014, **16**, 654–671.

90 C. M. Sharpless, M. Aeschbacher, S. E. Page, J. Wenk, M. Sander and K. McNeill, Photooxidation-induced changes in optical, electrochemical, and photochemical properties of humic substances, *Environ. Sci. Technol.*, 2014, **48**, 2688–2696.

91 J. Criquet, E. M. Rodriguez, S. Allard, S. Wellauer, E. Salhi, C. A. Joll and U. von Gunten, Reaction of bromine and chlorine with phenolic compounds and natural organic matter extracts - Electrophilic aromatic substitution and oxidation, *Water Res.*, 2015, **85**, 476–486.

92 A. A. Andrew, R. Del Vecchio, Y. Zhang, A. Subramaniam and N. V. Blough, Are Extracted Materials Truly Representative of Original Samples? Impact of C18 Extraction on CDOM Optical and Chemical Properties, *Front. Chem.*, 2016, **4**, 1–12.

93 M. Gonsior, J. Valle, P. Schmitt-Kopplin, N. Hertkorn, D. Bastviken, J. Luek, M. Harir, W. Bastos and A. Enrich-Prast, Chemodiversity of dissolved organic matter in the Amazon Basin, *Biogeosciences*, 2016, **13**, 4279–4290.

94 D. Schleheck, T. P. Knepper, K. Fischer and A. M. Cook, Mineralization of individual congeners of linear alkylbenzenesulfonate by defined pairs of heterotrophic bacteria, *Appl. Environ. Microbiol.*, 2004, **70**, 4053–4063.

95 M. Gonsior, M. Zwartjes, W. J. Cooper, W. Song, K. P. Ishida, L. Y. Tseng, M. K. Jeung, D. Rosso, N. Hertkorn and P. Schmitt-Kopplin, Molecular characterization of effluent organic matter identified by ultrahigh resolution mass spectrometry, *Water Res.*, 2011, **45**, 2943–2953.

96 V. Gomez, L. Ferreres, E. Pocurull and F. Borrull, Determination of non-ionic and anionic surfactants in environmental water matrices, *Talanta*, 2011, **84**, 859–866.

97 A. R. Ravishankara, Y. Rudich, R. Talukdar and S. B. Barone, Oxidation of atmospheric reduced sulphur compounds: Perspective from laboratory studies, *Philos. Trans. R. Soc., B*, 1997, **352**, 171–182.

98 S. Ding, F. Wang, W. Chu, C. Fang, E. Du, D. Yin and N. Gao, Effect of reduced sulfur group on the formation of CX3R-type disinfection by-products during chlor(am)ination of reduced sulfur compounds, *Chem. Eng. J.*, 2019, **361**, 227–234.

99 D. Tang, K. W. Warnken and P. H. Santschi, Organic complexation of copper in surface waters of Galveston Bay, *Limnol. Oceanogr.*, 2001, **46**, 321–330.

100 X. L. Armesto, L. M. Canle, M. I. Fernández, M. V. García and J. A. Santaballa, First steps in the oxidation of sulfur-containing amino acids by hypohalogenation: Very fast generation of intermediate sulfenyl halides and halosulfonium cations, *Tetrahedron*, 2000, **56**, 1103–1109.

101 J. A. Leenheer, R. L. Wershaw and M. M. Reddy, Strong-Acid, Carboxyl-Group Structures in Fulvic Acid from the Suwannee River, Georgia. 1. Minor Structures, *Environ. Sci. Technol.*, 1995, **29**, 393–398.

102 T. Krause, C. Tubbesing, K. Benzing and H. F. Schöler, Model reactions and natural occurrence of furans from hypersaline environments, *Biogeosciences*, 2014, **11**, 2871–2882.

103 D. H. Nam, B. J. Taitt and K. S. Choi, Copper-Based Catalytic Anodes to Produce 2,5-Furandicarboxylic Acid, a Biomass-Derived Alternative to Terephthalic Acid, *ACS Catal.*, 2018, **8**, 1197–1206.

104 M. Reichert, The Utilization of Liquid Chromatography Tandem Mass Spectrometry and Related Techniques for the Analysis and Identification of Emerging Contaminants in Aqueous Matrices, *PhD thesis*, Loyola University Chicago, 2016.

105 D. Zahn, T. Frömel and T. P. Knepper, Halogenated methanesulfonic acids: A new class of organic micropollutants in the water cycle, *Water Res.*, 2016, **101**, 292–299.

106 A. Raja, C. Vipin and A. Aiyappan, Biological importance of Marine Algae - An overview, *Int. J. Curr. Microbiol. Appl. Sci.*, 2013, **2**, 222–227.

107 M. Lukasova, J. Hanson, S. Tunaru and S. Offermanns, Nicotinic acid (niacin): New lipid-independent mechanisms of action and therapeutic potentials, *Trends Pharmacol. Sci.*, 2011, **32**, 700–707.

108 T. N. Makar'eva, A. I. Kalinovskii, V. A. Stonik and E. V. Vakhrusheva, Identification of 5-hydroxypicolinic acid among the products biosynthesized by Nocardia sp., *Chem. Nat. Compd.*, 1989, **25**, 125–126.

109 B. Zhang, Q. Xian, T. Gong, Y. Li, A. Li and J. Feng, DBPs formation and genotoxicity during chlorination of pyrimidines and purines bases, *Chem. Eng. J.*, 2017, **307**, 884–890.

110 E. Agus and D. L. Sedlak, Formation and fate of chlorination by-products in reverse osmosis desalination systems, *Water Res.*, 2010, **44**, 1616–1626.

111 S. Giller, F. Le Curieux, F. Erb and D. Marzin, Comparative genotoxicity of halogenated acetic acids found in drinking water, *Mutagenesis*, 1997, **12**, 321–328.

112 B. A. Poulin, J. N. Ryan, K. L. Nagy, A. Stubbins, T. Dittmar, W. Orem, D. P. Krabbenhoft and G. R. Aiken, Spatial Dependence of Reduced Sulfur in Everglades Dissolved Organic Matter Controlled by Sulfate Enrichment, *Environ. Sci. Technol.*, 2017, **51**, 3630–3639.